transitions of type $1^+ \rightarrow 2^+$(one-phonon) are 2–10 times slower than the $1^+ \rightarrow 0^+$ ground-state transitions,[11] an effect that is usually attributed to the collective vibrational character of the 2^+ state. However, in the $^{100}Tc \rightarrow ^{100}Ru$ decay, the reduced transition probability to the first 2^+ state is $\approx$100 times less than that to the ground state. Similarly, the transition probability to the second 0^+ level (1130 keV) is $\approx$100 times greater than that to the second 2^+ level (1362 keV). Since, in the vibrational-model description, both of these latter two levels are two-phonon states, it is clear that the dissimilar branching is not attributable to a simple difference in vibrational character. We suspect that a satisfactory explanation of the highly retarded decay to the first two 2^+ levels will need to take into consideration the detailed shell-model configurations of both the parent and daughter states.

ACKNOWLEDGMENTS

We are indebted to E. B. Shera and R. K. Sheline for helpful discussions and comments on the manuscript. Illuminating comments were also received from G. Scharff-Goldhaber and J. B. Ball. Finally, we wish to thank the LASL cyclotron staff for providing the proton-bombardment facilities.

PHYSICAL REVIEW VOLUME 187, NUMBER 4 20 NOVEMBER 1969

Level Scheme of ^{153}Sm Based on (n, γ), (n, e^-), and β-Decay Experiments*

R. K. SMITHER AND E. BIEBER†
Argonne National Laboratory, Argonne, Illinois 60439
AND
T. VON EGIDY AND W. KAISER
Physik-Department der Technischen Hochschuld München, München, Germany
AND
K. WIEN
Institut für Technische Kernphysik der Technischen Hochschule Darmstadt, Darmstadt, Germany
(Received 29 May 1969)

The $^{152}Sm(n, \gamma)^{153}Sm$ spectrum was measured with the Argonne bent-crystal spectrometer and with a Ge(Li) detector at the in-pile facility at the Argonne CP-5 research reactor. The low-energy bent-crystal spectrum consisted of 251 γ transitions associated with thermal-neutron capture in ^{152}Sm, with energies between 28 and 1041 keV. The γ-ray intensities were normalized to the previously established intensity of the 103-keV line in ^{153}Eu from the β decay of ^{153}Sm. The energies and intensities of 24 other lines associated with this β decay are also given. The high-energy (n, γ) spectrum, containing 23 lines between 4.5 and 5.9 MeV, was obtained with a Ge(Li) detector. The neutron binding energy of ^{153}Sm was found to be 5869.3$\pm$2.0 keV. The conversion-electron spectrum, measured with the high-resolution magnetic spectrometer at Munich, was used to obtain K and L conversion coefficients and corresponding multipole assignments for 37 of the low-energy γ transitions. The γ spectrum in ^{153}Sm following β decay of ^{153}Pm was measured with Ge(Li) and Si(Li) detectors. The source was made at Darmstadt through the $^{154}Sm(\gamma, p)^{153}Pm$ reaction. The (n, γ), (n, e^-), and β-decay experiments were combined to develop the level scheme of ^{153}Sm, in which unique spin and parity assignments are made for 13 of the 28 levels below 750 keV. The energy (keV) and J^π of the first 28 levels are: 0.000, $\frac{3}{2}^+$; 7.535, $\frac{5}{2}^+$; 35.843, $\frac{3}{2}^-$; 53.533, $\frac{7}{2}^+$ or $(\frac{5}{2}^+)$; 65.475, $\frac{9}{2}^+$ or $\frac{7}{2}^+$ or $\frac{5}{2}^+$; 90.874, $\frac{5}{2}^-$; 112.954, $\frac{9}{2}^+$ or $\frac{7}{2}^\pm$ or $\frac{5}{2}^\pm$; 127.298, $\frac{3}{2}^-$; 174.17, $\frac{7}{2}^-$; 182.90, $\frac{5}{2}^-$; (194.65), $\frac{5}{2}^\pm$ or $\frac{7}{2}^+$; 262.33, $\frac{7}{2}^+$ or $(\frac{5}{2}^+)$; (265.93), $\frac{7}{2}^-$ or $(\frac{5}{2}^\pm)$; 276.71, $\frac{3}{2}^+$; 321.11, $\frac{3}{2}^+$; 356.69, $\frac{5}{2}^+$; 362.29, $\frac{5}{2}^+$; (371.04), $\frac{9}{2}$ or $\frac{7}{2}$; 405.46, $\frac{3}{2}^-$; 414.91, $\frac{1}{2}^+$ or $\frac{3}{2}^+$; 447.07, $\frac{5}{2}$ or $\frac{7}{2}$; 450.04, $\frac{5}{2}$ or $\frac{7}{2}$; 481.08, $\frac{3}{2}^+$; 524.36, $\frac{5}{2}$; 630.20, $\frac{3}{2}^{(-)}$; 695.83, $\frac{1}{2}^{(+)}$ or $\frac{3}{2}^{(+)}$; 734.90, $\frac{5}{2}$; and 750.32, $\frac{1}{2}$ or $\frac{3}{2}$. The parentheses around a level energy or spin assignment mean that this value is less well established or is less probable if there is a choice. Of special interest is the very low-energy (7.53 keV) first excited state with $J^\pi = \frac{5}{2}^+$, which appears to be the second member of the strongly distorted ground-state rotational band. A good match between the theoretical predictions of the Nilsson model and the observed γ-ray branching ratio was obtained when nine of the eleven levels below 200 keV were assigned to a positive-parity, $K = \frac{3}{2}$, ground-state rotational band and two negative-parity, $K = \frac{3}{2}$, rotational bands with band heads at 35.84 and 127.30 keV.

I. INTRODUCTION

THE level scheme of ^{153}Sm is of special interest because this nucleus falls in the transition region between groups of nearly spherical nuclei ($A \leq 150$) and deformed nuclei ($A \geq 154$). The level schemes of the two adjacent even-Z, even-N nuclei, ^{152}Sm and ^{154}Sm, exhibit distorted but easily recognized ground-state rotational bands which suggest moderately strong deformations for these nuclei. The ^{153}Sm nucleus is in fact the lightest even-Z, odd-N samarium isotope that can, with reasonable certainty, be expected to exhibit a level scheme consistent with the Nilsson model for an

* Work performed in part under the auspices of the U.S. Atomic Energy Commission.
† Present address: Carl Zeiss, Inc., New York, New York.

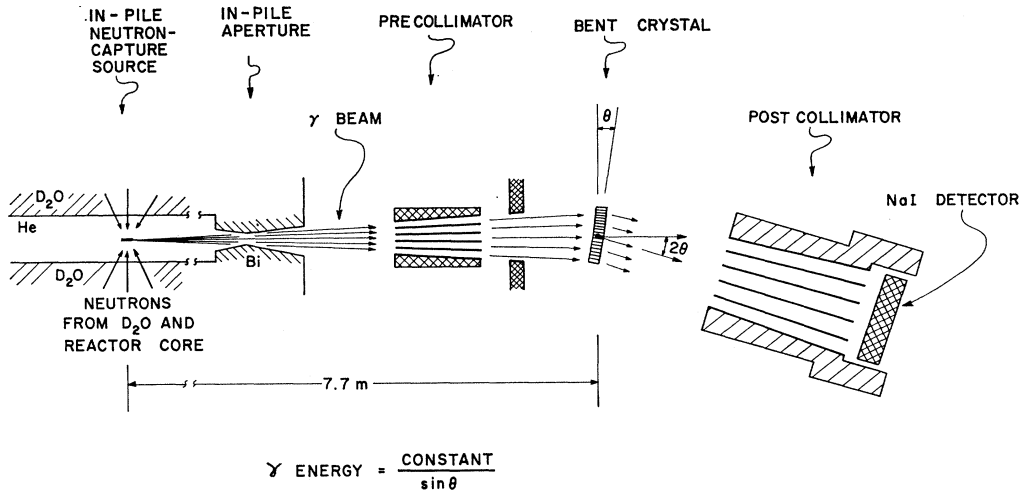

FIG. 1. Diagram of the bent-crystal spectrometer with the multislit precollimator in place. The γ rays result from neutron capture in a small sample at the left, near the core of the reactor. They emerge from the reactor through a Bi aperture and pass through the precollimator and a second aperture. A narrow energy increment of this γ beam is then diffracted by the (310) planes of the bent crystal, separated from the undiffracted beam by the post-collimator, and finally detected by a bank of 10 NaI crystals.

odd neutron coupled to a deformed core. The next lightest odd-A Sm, ^{151}Sm, falls between ^{152}Sm and ^{150}Sm, whose level schemes differ drastically (one is rotational, the other is vibrational or quasirotational[1]). It is hoped that a better understanding of the level scheme of ^{153}Sm will suggest an interpretation for the level scheme of ^{151}Sm, which is very similar in level structure. Both have many low-lying states which may or may not be members of rotational bands.[2–5]

Previously published charged-particle work[6–8] on the level schemes of the Sm isotopes suggests the existence of special states (either spherical or deformed) that can be followed from nucleus to nucleus through the transition region. This identification leads to the assignment of both spherical and deformed states in the same nucleus. Thus the ground state of one nucleus becomes the excited state of its neighbor and vice versa. An interesting example of this approach is the (p, p') work of Bassani *et al.*,[8] who report that they have followed a single-particle $\frac{3}{2}^-$ state through the level schemes from ^{147}Sm through ^{149}Sm and ^{151}Sm and into ^{153}Sm. As we shall see in the later discussion, their extrapolation falls right on a $\frac{3}{2}^-$ state in our final level scheme of ^{153}Sm, which we interpret as the $\frac{3}{2}^-$ band head of a $K=\frac{3}{2}$, [532] rotational band.

In our work, a series of (n, γ), (n, e^-), and β-decay studies are combined to develop the level scheme of ^{153}Sm. The very high resolution of the bent-crystal spectrometer at low γ energies and of the Ge(Li) detector at high energies were essential to the unraveling of this very complicated level scheme. Parity assignments were made for 20 of 27 levels identified in the level scheme below 750 keV and unique-spin assignments (13 levels) or a limited choice of assignments (usually only two values for the spin) were made for 39 levels identified below 1.4 MeV. A special effort was made to identify as many of the γ-ray transitions as possible so that the details of the γ-ray branching ratios of each level could be compared with theory. This last point proved important since one of the most interesting features of the proposed level scheme is that most of the γ-decay branching ratios of the 11 levels below 200-keV excitation energy can be explained in terms of the Nilsson model[9] for an odd neutron coupled to a deformed core. A number of preliminary reports have been made on this work.[10–14]

[1] E. Ya. Lure, L. K. Peker, and P. T. Prokof'ev, Izv. Akad. Nauk SSSR, Ser. Fiz. **32**, 74 (1968).
[2] B. Harmatz, T. H. Handley, and J. W. Mihelich, Phys. Rev. **128**, 1186 (1962).
[3] D. G. Burke, M. E. Law, and M. W. Johns, Can. J. Phys. **41**, 57 (1963).
[4] U. Bertelsen, G. T. Ewan, and H. L. Nielsen, Nucl. Phys. **50**, 657 (1964).
[5] P. Locard, J. Berthier, and J. C. Hocquenghem, Nucl. Phys. **89**, 497 (1966).
[6] S. Hinds, J. H. Bjerregaard, O. Hansen, and O. Nathan, Phys. Letters **14**, 48 (1965).
[7] R. A. Kenefick and R. K. Sheline, Phys. Rev. **139**, B1479 (1965).
[8] G. Bassani, Y. Cassagnon, C. Levi, and L. Papineau, in *Isobaric Spin in Nuclear Physics*, edited by J. D. Fox and D. Robson (Academic Press Inc., New York, 1966), paper C10.
[9] S. G. Nilsson, Kgl. Danske Videnskab. Selskab, Mat.-Fys. Medd. **29**, No. 16 (1955).
[10] R. K. Smither, E. Bieber, T. V. Egidy, W. Kaiser, and K. Wien, Bull. Am. Phys. Soc. **12**, 1065 (1967).
[11] T. v. Egidy, H. F. Mahlein, W. Kaiser, B. C. Dutta, A. Jones, and A. A. Suarez, in Proceedings of the Topical Conference for Neutron Physics at Reactors Julich, 1967 (unpublished).
[12] R. K. Smither, E. Bieber, T. V. Egidy, W. Kaiser, and K. Wien, in Argonne National Laboratory Report No. ANL-7481, 1968, p. 20 (unpublished).
[13] T. v. Egidy, Konversionelektronen nach dem Neutroneneinfang, Habilitationsschrift, Technische Hochschule München, 1968 (unpublished).
[14] Nuclear Data Tables **5A**, 139 (1968).

TABLE I. Isotopic abundances in the (n, γ) sample used in the bent-crystal and Ge(Li) experiments.

Isotope	^{144}Sm	^{147}Sm	^{148}Sm	^{149}Sm	^{150}Sm	^{152}Sm	^{154}Sm
Abundance (%)	<0.02	0.19	0.07	0.11	0.09	99.06	0.48
σ (barns)	0.7	90		64 000[a]	100	210	5
$\sigma\times$abundance (barns$\times$%)	<0.014	17		7 040	9	20 800	2.5

[a] Effective cross section for the reactor neutron spectrum taken from Ref. 20.

A level scheme with rotational bands and Nilsson assignments was constructed by Kenefick and Sheline[7] in 1965 using (d, p) data. Our results verify only one of their rotational bands and disprove most of their spin and parity predictions. This shows the necessity to complement charged-particle-reaction data with detailed decay studies. The more recent level scheme of Sheline[15] which is based on further (d, p) and (d, t) measurements and on our preliminary spin and parity assignments[10] is in much better agreement with the present results.

II. EXPERIMENTAL METHOD

A. Bent-Crystal Spectrometer Data

The low-energy (n, γ) spectrum was measured with the 7.7-m Argonne bent-crystal spectrometer.[16–18] (Fig. 1). The neutron flux at the target was 3×10^{13} neutrons/cm^2 sec. Three samples with different enrichments were used to identify γ rays from the ^{149}Sm$(n, \gamma)^{150}$Sm, ^{150}Sm$(n, \gamma)^{151}$Sm, and ^{152}Sm$(n, \gamma)^{153}$Sm reactions.[19] The isotopic composition of the sample enriched to 99% in ^{152}Sm (the one used primarily in this publication) appears in Table I. This sample consisted of 180 mg of Sm_2O_3 enclosed in an Mg(85%)-Al(15%) holder which constrained the sample to a volume 7 cm high, 1 cm deep, and 0.017 cm wide and formed a narrow line source for the bent-crystal spectrometer (Fig. 1). The ^{149}Sm$(n, \gamma)^{150}$Sm γ spectrum has been published[20]; the information on the ^{150}Sm$(n, \gamma)^{151}$Sm and ^{151}Sm$(n, \gamma)^{152}$Sm reactions will be published at a later date.

The precision energies and intensities of the 251 γ rays identified with the ^{152}Sm$(n, \gamma)^{153}$Sm reaction appear with their errors in columns 1–4 of Table II. Each energy and intensity is an average taken from the analysis of a series of 4–10 runs over the spectrum obtained with the sample enriched in ^{152}Sm. The analyses were done either by hand or with a computer. In cases of complex structure, the computer analysis was used.

An example of the bent-crystal spectrometer data appears in Fig. 2. It consists of γ-ray counting rates as a function of Bragg angle (which has been converted into γ energy for the convenience of the reader). The lower section (B) shows the quality of the data[16–18,20]

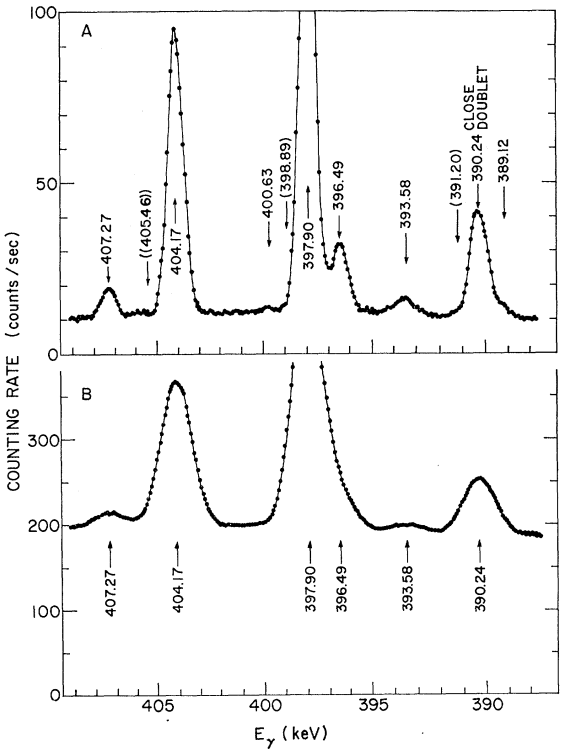

FIG. 2. A comparison between data obtained with the bent-crystal spectrometer after (curve A) and before (curve B) the installation of the thinner bent crystal and the multislit precollimator. Both curves represent the 390–410-keV region of the ^{152}Sm (n, γ) ^{153}Sm spectrum; the counting rate plotted is that in 10% of the aperture of the bent crystal—i.e., in one of the 10 NaI crystals in the detector bank. In an attempt to obtain statistics good enough that the doublet at 397.90 and 396.49 keV could be resolved by line-shape analysis, a long counting time was used for each point of the "before" spectrum. Although the counting time per point was only 1/25 as large for the after spectrum as for the before, the after spectrum obviously is far superior for this purpose.

[15] R. K. Sheline (private communication); in Proceedings of the International Conference on Nuclear Physics at Dubna, 1968 (unpublished).

[16] R. K. Smither, in *Proceedings of the International Conference on Nuclear Physics with Reactor Neutrons*, edited by F. E. Throw (Argonne National Laboratory, Argonne, Ill., 1963), p. 89.

[17] R. K. Smither, California Institute of Technology Report, Pasadena, Calif. 1964, p. 9 (unpublished).

[18] R. K. Smither, in Argonne National Laboratory Report No. ANL-6789, p. 14 (unpublished).

[19] The isotopically enriched samples were obtained from the Isotope Division of Oak Ridge National Laboratory.

[20] R. K. Smither, Phys. Rev. **150**, 964 (1966).

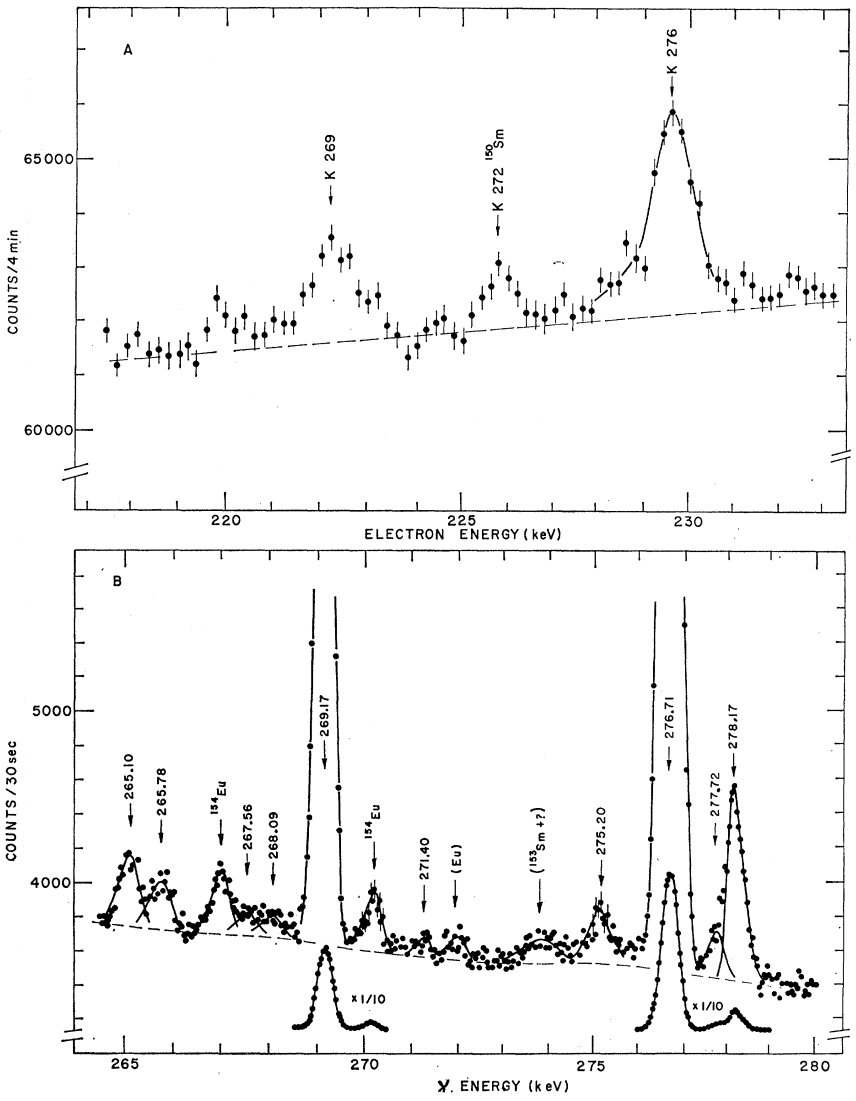

FIG. 3. A comparison of the conversion-electron data (curve A) with the bent-crystal data (curve B) for the γ energy region from 265 to 280 keV. The upper plot (curve A) shows a typical conversion-electron run with a 4-min counting time at each point. The lower plot (curve B) shows the raw data taken in one of the 10 NaI detectors in the bent-crystal detector banks, with a 30-sec counting time at each point. The notations $K269$ and $K276$ in plot A are used to indicate the K conversion lines of the 269- and 276-keV γ rays from the ^{152}Sm (n, γ) ^{153}Sm reaction. The $K272$ ^{150}Sm indicates the position of a similar line from the ^{149}Sm (n, γ) ^{150}Sm reaction. The lines in the bent-crystal data (plot B) associated with the ^{153}Sm level scheme are labeled with their measured γ energies. The ^{154} Eu and (Eu) labels indicate lines associated with europium level schemes.

taken in the spring of 1964 with the old spectrometer system, while the upper section (A) shows the same region of the spectrum taken with the new spectrometer system[21] in the spring of 1968. In the unraveling of this complex spectrum, the usefulness of the new data taken with better resolution and improved peak-to-background ratio is obvious. This was particularly true when trying to set upper limits on the intensities of "missing" lines (i.e., unobserved transitions that one might expect to exist on the basis of the proposed decay scheme). An example of this is given in Fig. 2, where the double parenthesis notation ((405.46)) indicates the position of a missing line.

In most of the runs, the counting rate was measured for 10–50 sec at each point with a step size of 0.5 sec of arc. The more recent work (1968) was done with a 2-mm-thick quartz crystal[22] measuring 30 cm on a side. The older work made use of a 4-mm-thick quartz crystal. When the 2-mm-thick bent crystal was used in first-order diffraction, using the (310) planes the line width ΔE_γ full width at half maximum (FWHM), (in keV) at a γ-ray energy E_γ (in MeV) was $\Delta E_\gamma = 4.5 E_\gamma^2$, which gives 4.5 keV at 1 MeV and 45 eV at 100 keV. The runs were analyzed individually first and then added together and reanalyzed to improve the sensitivity for weak lines. In many cases in which questions arose concerning energies and intensities of weak lines, special experiments were performed to improve the sensitivity or energy precision of the γ-ray measurements. This additional work causes some variation in

[21] R. K. Smither and D. J. Buss, in Argonne National Laboratory Report No. ANL-7512, 1968, pp. 4–7 (unpublished); Argonne National Laboratory Report No. ANL-7481, 1968, p. 15 (unpublished).

[22] The quartz crystal was cut and polished by Hilger and Watts of England.

TABLE II. Combination of the bent-crystal-spectrometer $^{152}Sm(n,\gamma)^{153}Sm$ data and the magnetic-spectrometer $^{152}Sm(n,e^-)^{153}Sm$ data on the low-energy region. Columns 1–4 give the γ energies E_γ and intensities I_γ with their corresponding errors, as obtained from the bent-crystal spectrometer. The γ intensities I_γ (γ rays per 100 neutron captures) were normalized so that the 103-keV line in ^{153}Eu was equal to 28.0 γ's per 100 neutron captures (Table III). All errors quoted on I_γ are errors on the intensity of the γ rays relative to this line and do not include any error from this normalization procedure (as explained in the text). The conversion-electron data are given in columns 5–10. E_e and I_e are the observed electron energy and intensity (electrons per 100 neutron captures). E_γ(ce) is the

Bent-crystal spectrometer				Conversion-electron spectrometer					
E_γ (keV)	ΔE_γ (keV)	I_γ γ rays/100n	$\Delta I_\gamma/I_\gamma$ (%)	E_γ(ce) (keV)	Electron shell	E_e (keV)	ΔE_e (keV)	I_e β rays/100n	$\Delta I_e/I_e$ (%)
(1)	(2)	(3)	(4)	(5)	(6)	(7)	(8)	(9)	(10)
7.535[a]					$L_{II\ III}$[b]			50.[b]	40
					M			<10.	
28.309	0.005	2.10	10		L_I	20.57[c]		<2.0	
					L_{II}	21.00[c]		<2.0	
					L_{III}	21.59[c]		<2.0	
35.571	0.005	0.030	10						
35.842	0.005	6.20	10	35.84	L_I	28.10	0.03	1.83	30
					L_{II}	25.53[c]		<1.0	
					L_{III}	26.12[c]		<1.2	
36.423	0.005	0.021	20		L_I	28.68[c]		<1.0	
					L_{II}	29.11[c]		<1.0	
					L_{III}	29.70[c]		<1.0	
37.343	0.005	0.223	10		L_I	29.60		<1.0	
					L_{II}	30.03		<1.0	
					L_{III}	30.62		<1.0	
45.996	0.005	0.262	10	46.03	L_I	38.14	0.05	1.5[d]	60
					L_{II}	38.64	0.05	1.6[d]	60
					L_{III}	39.31	0.05	2.5[d]	40
51.040	0.010	0.030	20						
53.534	0.005	0.136	10	53.56	L_I	45.60	0.2	0.35[e]	60
					L_{II}	46.24	0.06	1.25[e]	20
					L_{III}	46.86	0.06	1.40[e]	20
55.031	0.008	0.171	10		K	8.19[c]		<1.7	
					L_I	47.29[c]		<0.3	
					L_{II}	47.72[c]		<0.3	
					L_{III}	48.44[c]		<0.3	
55.61	0.01	0.029	20		K	8.77[c]		<1.7	
					L_I	47.87[c]		<0.3	
					L_{II}	48.30[c]		<0.3	
					L_{III}	49.02[c]		<0.3	
57.94	0.01	0.042	20		K	11.10[c]		$0.13<I_e<1.5$	
					L_I	50.20[c]		$0.07<I_e<0.3$	
					L_{II}	50.63[c]		$0.07<I_e<0.3$	
					L_{III}	51.22[c]		$0.07<I_e<0.3$	
59.42	0.01	0.026	20		K	12.58[c]		<1.5	
					L_I	51.68[c]		<0.3	
					L_{II}	52.11[c]		<0.3	
					L_{III}	52.70[c]		<0.3	
63.66	0.01	0.007	50						
66.16	0.01	0.008	30						
76.96	0.01	0.043	20						
79.43	0.01	0.021	20						
83.03	0.02	0.043	20						
83.302	0.008	0.059	20						
83.339	0.005	1.70	6	83.35	K	36.3	0.3	0.7	30
					L_I	75.61	0.06	0.13[f]	50

corresponding γ energy derived from the conversion-electron data and can be compared with the E_γ of the bent-crystal spectrometer in column 1. The experimental conversion coefficients I_e/I_γ appear in column 11 and are followed in columns 13–15 by the theoretical conversion coefficients for $E1$, $E2$, and $M1$. Column 16 gives the multipole assignment derived from the conversion coefficient. The checks in column 17 indicate that the γ is used in the level scheme. Two checks indicate that it was used twice, etc. All intensity errors are given as a percentage of the quoted value. The fractional error $\Delta(I_e/I_\gamma)/(I_e/I_\gamma)$ is given in percent (column 12).

Conversion coefficients: Experimental I_e/I_γ (11)	Experimental $\Delta(I_e/I_\gamma)/(I_e/I_\gamma)$ (12)	Theoretical $E1$ (13)	Theoretical $E2$ (14)	Theoretical $M1$ (15)	Multipolarity of γ (16)	In-level scheme (17)	Remarks (18)
		38.	3×10^5	45.	$(M1+E2)$	√	
		10.	7×10^4	97.			
<1.0		0.51	1.1	7.5	$E1$	√	
<1.0		0.23	165.	0.68			
<1.0		0.43	226.	0.13			
						√	
0.30	33	0.30	0.56	3.80	$E1$	√	
<0.16		0.14	53.5	0.35			
<0.20		0.20	71.8	0.07			
<48.		0.29	0.55	3.63	$(E1, M1)$	√	
<48.		0.13	49.5	0.33			
<48.		0.19	66.2	0.06			
<4.4		0.27	0.54	3.37	$(E1, M1)$	√	
<4.4		0.12	43.7	0.30			
<4.4		0.17	58.2	0.06			
5.7	65	0.16	0.45	1.82	$M1+$	√	
6.1	65	0.06	15.7	0.16	$(50\pm30)\%E2$		I_e-KLX (Auger)[d]
9.6	45	0.08	19.9	0.03			
							Questionable isotopic assignment
2.6	65	0.113	0.38	1.16	$E2+$	√	
9.2	25	0.037	7.53	0.101	$<25\%\ M1$		I_e+KMN, KNN (Auger)[e]
10.3	25	0.050	9.23	0.019			
<10.		1.15	5.32	8.07	$(M1, E1)$	√	
<1.7		0.105	0.36	1.07	$<25\%\ E2$		
<1.7		0.033	6.60	0.093			
<1.7		0.046	8.02	0.017			
<60.		1.12	5.18	7.83	$E1, M1, E2$	√	
<10.		0.103	0.36	1.04			
<10.		0.032	6.28	0.090			
<10.		0.044	7.61	0.017			
$3<I_e/I_\gamma<36$		1.00	4.67	6.96	$E2, M1$	√	Lower limit on I_e
$1.5<I_e/I_\gamma<11$		0.093	0.33	0.92			and I_e/I_γ apply
$1.5<I_e/I_\gamma<11$		0.028	5.18	0.079			only to $E1$
$1.5<I_e/I_\gamma<11$		0.038	6.20	0.015			transitions
<60.		0.939	4.38	6.47	$E1, M1, E2$	√	
<11.		0.087	0.32	0.86			
<11.		0.026	4.60	0.073			
<11.		0.035	5.47	0.014			
							Questionable isospin assignment
						√	Quest. iso. assign.
						√	
						√	
						√	
0.41	32	0.380	1.87	2.43	$E1$	√	
0.076	60	0.038	0.166	0.32			$(I_e-L_2 83\text{Eu})$[f]

TABLE II

Bent-crystal spectrometer				Conversion-electron spectrometer					
E_γ (keV)	ΔE_γ (keV)	I_γ γ rays/100n	$\Delta I_\gamma/I_\gamma$ (%)	E_γ(ce) (keV)	Electron shell	E_e (keV)	ΔE_e (keV)	I_e β rays/100n	$\Delta I_e/I_e$ (%)
(1)	(2)	(3)	(4)	(5)	(6)	(7)	(8)	(9)	(10)
88.16	0.01	0.0073	30						
90.56	0.01	0.052	20						
90.766	0.013	0.116	20						
90.874	0.005	2.47	5	90.92	K	44.08	0.07	1.33[g,e]	35
91.455	0.005	0.80	5	91.47	K	44.63	0.05	2.45[e]	35
					L_{I}	83.59	0.2	0.30	50
92.03	0.01	0.08	15		K	45.19[c]		<0.4	
					L_{I}	84.29[c]		<0.1	
					L_{II}	84.72[c]		<0.1	
					L_{III}	85.44[c]		<0.1	
93.81	0.01	0.008	30						
104.58	0.01	0.008	30						
104.93	0.01	0.007	40						
105.42	0.01	0.016	20		K	58.58[c]		<0.2	
					L_{I}	97.68[c]		<0.1	
					L_{II}	98.11[c]		<0.1	
					L_{III}	98.83[c]		<0.1	
108.71	0.01	0.250	6		K	61.78[c]		<0.3	
					L_{I}	100.97[c]		<0.1	
					L_{II}	101.40		<0.1	
					L_{III}	102.12		<0.1	
108.89	0.01	0.051	10						
112.65	0.01	0.018	15						
113.18	0.01	0.010	15						
117.330	0.005	0.014	15						
118.838	0.005	0.120	7						
119.763	0.005	2.84	5	119.76[h]	K	72.92	0.05	0.43	10
					L_{I}	112.12	0.10	0.078	20
120.64	0.01	0.130	7		K	73.80[c]		<0.2	
					L_{I}	112.90[c]		<0.03	
123.62	0.02	0.029	15						
126.44	0.02	0.012	30						
127.298	0.005	6.60	5	127.30[h]	K	80.46	0.05	0.93	6
					L_{I}	(119.76)[f]	0.05	0.11	20
129.36	0.01	0.69	5		K	82.52[c]		<0.12	
135.54	0.02	0.028	15						
138.21	0.02	0.024	15						
138.32	0.02	0.035	15		K	91.48[c]		<0.1	
138.64	0.03	0.015	10						
146.73	0.04	0.016	20						
147.06	0.01	0.242	10	147.4	K	100.6	0.4	0.15	30
149.417	0.011	0.025	10						
162.09	0.02	0.027	20						
163.21	0.02	0.011	40						
166.64	0.01	0.78	5	166.60	K	(119.76)[i]	0.05	0.065[f]	20
167.15	0.03	0.008	40						
170.33	0.03	0.013	33						
171.45	0.01	0.069	10						
173.34	0.01	0.137	8		K	126.50[c]		<0.02	
173.70	0.01	0.014	25						
175.370	0.011	1.21	5	175.38	K	128.54	0.05	0.073	10
180.34	0.03	0.011	20						

(*Continued*)

Conversion coefficients							
Experimental		Theoretical			Multipolarity	In-level	
I_e/I_γ	$\Delta(I_e/I_\gamma)/(I_e/I_\gamma)$	$E1$	$E2$	$M1$	of γ	scheme	Remarks
(11)	(12)	(13)	(14)	(15)	(16)	(17)	(18)
						√	
						√	Quest. iso. assign.
0.54	40	0.301	1.50	1.89	$E1$	√	I_e+M46 keV[g] $+KMM$ (Auger)[e]
3.08	40	0.296	1.48	1.86	$M1(E2+E_0)$	√	
0.38	50	0.030	0.133	0.244			
<5.0		0.291	1.46	1.83	$E1, M1, E2$	√	
<1.2		0.030	0.131	0.239			
<1.2		0.006	0.586	0.020			
<1.2		0.008	0.619	0.004			
						√	
							Quest. iso. assign.
							Quest. iso. assign.
<12.5		0.202	1.02	1.24	$E1, M1, E2$	√	
<6.3		0.021	0.094	0.162			
<6.3		0.004	0.309	0.013			
<6.3		0.005	0.315	0.002			
<1.2		0.186	0.937	1.13	$E1, M1, E2$	√	
<0.4		0.019	0.086	0.148			
<0.4		0.036	0.269	0.012			
<0.4		0.045	0.271	0.002			
							Quest. iso. assign.
							Quest. iso. assign.
							Quest. iso. assign.
0.150	12	0.143	0.709	0.860	$E1$	√	
0.027	20	0.015	0.066	0.112			
<1.5		0.140	0.694	0.843	$E1, M1, E2$	√	
<0.23		0.015	0.065	0.109			
						√	
0.140	10	0.121	0.595	0.724	$E1$	√	
0.017	25	0.013	0.056	0.094			I_e-K166[f]
<0.18		0.116	0.567	0.692	$E1$	√	
						√√	
<2.9		0.097	0.463	0.574	$E1, M1, E2$	√	
						√	
0.62	35	0.082	0.385	0.483	$M1, E2$	√	
						√	
						√	
0.083	22	0.059	0.263	0.342	$E1$	√	I_e-L127[f] Composite with an impurity line
						√	
						√	
<0.15		0.053	0.233	0.307	$E1$	√	
						√	
0.060	12	0.052	0.225	0.297	$E1$	√	

TABLE II

Bent-crystal spectrometer				Conversion-electron spectrometer					
E_γ (keV)	ΔE_γ (keV)	I_γ γ rays/100n	$\Delta I_\gamma/I_\gamma$ (%)	E_γ(ce) (keV)	Electron shell	E_e (keV)	ΔE_e (keV)	I_e β rays/100n	$\Delta I_e/I_e$ (%)
(1)	(2)	(3)	(4)	(5)	(6)	(7)	(8)	(9)	(10)
181.80	0.03	0.011	20						
182.44	0.02	0.010	25						
182.52	0.01	0.024	15						
182.900	0.008	1.49	5	182.91	K	136.07	0.05	0.066	15
184.82	0.02	0.044	20						
185.845	0.011	0.056	10						
187.10	0.02	0.008	20						
188.119	0.011	0.028	10						
193.82	0.02	0.060	15						
194.33	0.02	0.063	15						
194.66	0.03	0.021	25						
194.95	0.04	0.014	30						
195.58	0.04	0.018	30						
194.80	0.04	0.018	30						
196.866	0.011	0.210	5		K	150.03[e]		<0.03	
198.20	0.04	0.009	30						
200.93	0.07	0.033	15						
202.78	0.05	0.011	20						
203.25	0.04	0.042	20						
204.36	0.03	0.070	8						
208.802	0.014	0.103	12						
211.24	0.02	0.020	15						
212.14	0.04	0.020	15						
212.844	0.011	0.150	6						
220.77	0.06	0.004	30						
222.656	0.011	0.244	8						
223.173	0.011	0.250	8	223.25	K	176.41[i]	0.2	0.056[j]	45
					L_{I}	215.59[i]	0.4	0.016[j]	60
229.40	0.05	0.0063	30						
230.243	0.013	0.015	12						
234.93	0.05	0.029	12						
240.868	0.014	0.047	15						
242.24	0.20	0.014	50						
243.06	0.04	0.037	15						
244.62	0.04	0.029	15						
247.08	0.03	0.030	15						
247.62	0.06	0.007	30						
248.39	0.04	0.014	15						
249.14	0.04	0.024	15						
249.73	0.04	0.015	15						
252.01	0.016	0.046	15						
254.794	0.015	0.449	5	255.03	K	208.19	0.1	0.042	35
257.68	0.05	0.027	20						
258.43	0.05	0.008	50						
261.15	0.05	0.0036	50						
261.58	0.03	0.055	12						
261.76	0.04	0.011	30						
262.31	0.04	0.0057	30						
262.86	0.04	0.014	22						
263.20	0.04	0.016	20						
264.25	0.05	0.008	40						
265.10	0.04	0.063	8						
265.78	0.04	0.043	12						
267.56	0.03	0.014	20						

(*Continued*)

Conversion coefficients							
Experimental		Theoretical			Multipolarity	In-level	
I_e/I_γ	$\Delta(I_e/I_\gamma)/(I_e/I_\gamma)$	$E1$	$E2$	$M1$	of γ	scheme	Remarks
(11)	(12)	(13)	(14)	(15)	(16)	(17)	(18)
							On wing of impurity line
						√	
0.044	18	0.046	0.198	0.265	$E1$	√	
						√	
						√	
						√	Possible doublet
						√	Doublet
						√	
							Quest. iso. assign.
							Quest. iso. assign.
							Quest. iso. assign.
<0.14		0.038	0.158	0.217	($E1$, $E2$)	√√	
							Quest. iso. assign.
						√	
						√	
						√	
0.22	35	0.0272	0.107	0.154	$M1$, $E2$	√	I_e-K223 Sm 150[j]
0.064	60	0.0031	0.011	0.020			I_e-L223 Sm 150[j]
						√	
						√	
						√	Doublet
						√	Poss. doublet
							Quest. iso. assign.
							Quest. iso. assign.
0.093	40	0.019	0.072	0.107	$E2$, $M1$	√	
						√√	
						√	
						√	

TABLE II

Bent-crystal spectrometer				Conversion-electron spectrometer					
E_γ (keV)	ΔE_γ (keV)	I_γ γ rays/100n	$\Delta I_\gamma/I_\gamma$ (%)	E_γ(ce) (keV)	Electron shell	E_e (keV)	ΔE_e (keV)	I_e β rays/100n	$\Delta I_e/I_e$ (%)
(1)	(2)	(3)	(4)	(5)	(6)	(7)	(8)	(9)	(10)
268.09	0.03	0.013	20						
269.17	0.02	0.786	6	269.09	K	(222.25)[i]	0.2	0.032[j]	50
					L_{I}	(261.79)[i]	0.3	0.010[j]	70
271.40	0.08	0.012	30						
275.20	0.04	0.037	15						
276.71	0.02	1.62	6	276.71	K	229.87	0.08	0.187	6
					L_{I}	269.5	0.3	0.023	40
277.72	0.04	0.044	12						
278.17	0.02	0.195	6	277.8	K	231.0	0.5	0.017	50
282.55	0.04	0.049	12						
284.41	0.05	0.013	30						
285.23	0.04	0.020	20						
287.49	0.06	0.030	15						
290.71	0.08	0.015	30						
291.17	0.05	0.090	10						
293.54	0.07	0.031	20						
296.82	0.05	0.028	15						
298.20	0.05	0.038	12						
298.94	0.03	0.075	8						
302.95	0.04	0.105	12	302.87	K	256.03	0.2	0.024	30
303.16	0.04	0.105	12						
307.21	0.04	0.928	25						
308.71	0.07	0.100	8						
310.62	0.07	0.019	20						
312.85	0.05	0.017	25						
313.54	0.03	0.235	6						
314.60	0.03	0.099	8						
315.21	0.05	0.053	10						
317.80	0.03	0.135	8						
321.13	0.03	2.64	6	321.11	K	274.27	0.08	0.171	6
326.45	0.05	0.031	15						
327.81	0.08	0.017	30						
329.39	0.03	0.186	7						
330.75	0.03	0.103	10						
340.95	0.05	0.071	10						
347.85	0.06	0.018	30						
349.16	0.05	0.117	8						
350.20	0.05	0.156	7						
351.19	0.06	0.051	11						
354.76	0.03	1.01	6	354.72	K	307.88	0.07	0.063[j]	20
356.62	0.10	0.038	25						
358.48	0.06	0.050	14						
359.12	0.10	0.032	16						
360.21	0.10	0.036	16						
362.30	0.03	0.810	7	362.30	K	315.46	0.12	0.041	40
365.13	0.07	0.034	20						
367.03	0.07	0.034	20						
368.27	0.10	0.082	10						
369.63	0.03	0.300	6						
370.43	0.09	0.028	30						
371.89	0.09	0.016	35						
372.87	0.04	0.075	10						
374.69	0.04	0.048	14						
379.10	0.04	0.132	8						
384.79	0.04	0.102	10						
386.02	0.07	0.021	30						

(*Continued*)

Conversion coefficients							
Experimental		Theoretical			Multipolarity	In-level	
I_e/I_γ	$\Delta(I_e/I_\gamma)/(I_e/I_\gamma)$	$E1$	$E2$	$M1$	of γ	scheme	Remarks
(11)	(12)	(13)	(14)	(15)	(16)	(17)	(18)
						√	
0.041	50	0.017	0.061	0.092	$E2, M1(E1)$	√	I_e-K269 Sm 150[j]
0.013	70	0.0019	0.0067	0.012			I_e-L269 Sm 150[j]
						√	
0.115	9	0.016	0.056	0.086	$M1(E2+E0)$	√	
0.014	40	0.0018	0.0062	0.0112			
0.087	50	0.015	0.055	0.085	$M1, E2$	√	
							Quest. iso. assign.
						√	
						√	
						√	
						√	
						√	
0.114	35	0.012	0.043	0.067	$M1$	Z	Close doublet
						√Z	
						√	
						√	
						√	
0.065	9	0.011	0.036	0.058	$M1$	√	
						√	
							Possible doublet
						√	
						√	
						√	
0.062	14	0.0083	0.027	0.045	$M1$	√	I_e-K356 Sm 150[j]
						√	Possible doublet
						√	
0.051	42	0.0079	0.025	0.042	$M1(E2)$	√	
						√	
						√	
						√	Possible doublet

TABLE II

Bent-crystal spectrometer				Conversion-electron spectrometer					
E_γ (keV)	ΔE_γ (keV)	I_γ γ rays/100n	$\Delta I_\gamma/I_\gamma$ (%)	E_γ(ce) (keV)	Electron shell	E_e (keV)	ΔE_e (keV)	I_e β rays/100n	$\Delta I_e/I_e$ (%)
(1)	(2)	(3)	(4)	(5)	(6)	(7)	(8)	(9)	(10)
389.12	0.16	0.054	30						
390.24	0.04	0.667	6		K	343.40[c]		<0.01	
393.58	0.08	0.109	10						
396.49	0.04	0.431	8						
397.90	0.04	3.31	6	397.76	K	350.92	0.16	0.021	16
398.89	0.08	0.051	20						
400.63	0.16	0.028	40						
404.17	0.04	1.85	6		K	357.33		<0.02	
407.30	0.07	0.171	8						
413.75	0.15	0.176	20						
414.97	0.06	3.04	6	414.96	K	368.12	0.10	0.107	10
417.13	0.17	0.021	40						
419.93	0.17	0.011	60						
422.71	0.09	0.024	40						
425.97	0.19	0.029	30						
428.18	0.19	0.024	40						
433.11	0.10	0.071	15						
435.43	0.20	0.028	30						
439.53	0.06	0.280	8						
442.51	0.06	0.754	6						
445.15	0.06	0.164	10						
447.27	0.06	0.050	16						
452.22	0.30	0.017	50						
456.20	0.30	0.018	50						
459.92	0.06	0.321	8						
470.65	0.06	1.86	7	471.08	K	424.24	0.4	0.016	35
473.63	0.06	2.23	7	473.76	K	426.92	0.3	0.037	15
481.14	0.06	0.686	8						
482.51	0.06	0.175	10						
488.57	0.12	0.135	11						
491.55	0.12	0.040	25						
494.35	0.12	0.098	20						
502.21	0.18	0.227	12						
503.52	0.18	0.075	20						
516.72	0.10	0.473	7						
518.02	0.13	0.115	16						
521.12	0.20	0.042	30						
523.06	0.20	0.104	20						
524.22	0.20	0.152	20						
530.65	0.26	0.059	40						
532.92	0.26	0.147	20						
535.42	0.28	0.137	25						
539.16	0.30	0.113	25						
540.53	0.30	0.125	25						
549.66	0.30	0.064	35						
551.74	0.30	0.095	25						
559.88	0.15	0.129	20						
561.61	0.22	0.052	25						
564.70	0.22	0.141	20						
567.50	0.15	0.524	12						
568.52	0.24	0.229	14						
574.05	0.50	0.101	30						
574.99	0.50	0.114	30						
579.91	0.50	0.155	25						
582.96	0.50	0.276	16						
586.44	0.50	0.270	16						
589.83	0.50	0.178	20						

(*Continued*)

Conversion coefficients							
Experimental		Theoretical			Multipolarity	In-level	
I_e/I_γ (11)	$\Delta(I_e/I_\gamma)/(I_e/I_\gamma)$ (12)	$E1$ (13)	$E2$ (14)	$M1$ (15)	of γ (16)	scheme (17)	Remarks (18)
<0.015		0.0066	0.021	0.035	($E1$)	√	Unresolved doublet
						√√	
						√	
0.0063	19	0.0063	0.021	0.033	$E1$	√	
<0.011		0.0061	0.019	0.032	$E1$		
						√	
						√	
0.035	14	0.0057	0.018	0.030	$M1$	√	
						√	Unresolved doublet
						√	
						√	
						√	
						√	
						√	
						√	
0.0086	38	0.0043	0.0125	0.0215	$E1$, $E2$		Possible doublet
0.017	20	0.0042	0.0123	0.0212	$M1$, $E2$	√√	
						√	
						√	
						√	
						√	
						√	
							Possible doublet
						√	
						√	
						√	
						√	
						√	
						√	
						√	
							Possible doublet
							Possible doublet

TABLE II

Bent-crystal spectrometer				Conversion-electron spectrometer					
E_γ (keV)	ΔE_γ (keV)	I_γ γ rays/100n	$\Delta I_\gamma/I_\gamma$ (%)	E_γ(ce) (keV)	Electron shell	E_e (keV)	ΔE_e (keV)	I_e β rays/100n	$\Delta I_e/I_e$ (%)
(1)	(2)	(3)	(4)	(5)	(6)	(7)	(8)	(9)	(10)
593.77	0.17	0.223	14						
604.19	0.34	0.073	30						
605.93	0.34	0.192	16						
610.07	0.28	0.030	50						
614.44	0.16	0.170	12						
618.94	0.40	0.095	30						
622.76	0.10	1.42	7						
627.55	0.30	0.363	12						
630.24	0.10	1.82	7		K	583.42		<0.015	
646.28	0.22	0.233	12						
649.77	0.33	0.090	35						
659.95	0.10	2.07	7		K	613.13		<0.015	
662.90	0.50	0.160	25						
675.28	0.33	0.161	25						
681.70	0.26	0.289	16						
689.41	0.35	0.257	16						
693.16	0.35	0.281	16						
698.41	0.24	0.353	14						
702.61	0.24	0.224	20						
707.08	0.25	0.229	20						
714.91	0.20	0.986	10						
721.96	0.50	0.096	40						
727.37	0.25	0.420	15						
734.89	0.13	1.65	10						
743.10	0.53	0.183	35						
746.70	0.53	0.239	30						
749.92	0.54	0.188	30						
753.60	0.27	0.546	10						
757.59	0.57	0.083	50						
767.62	0.24	0.685	10						
772.31	0.30	0.406	16						
780.72	0.24	0.535	12						
788.72	0.24	0.985	10						
808.40	0.33	0.263	20						
817.44	0.66	0.101	50						
825.20	0.34	0.492	16						
834.07	0.34	0.483	16						
838.98	0.34	0.870	12						
847.15	0.70	0.185	50						
858.02	0.70	0.229	30						
871.28	0.51	0.276	30						
878.63	0.38	0.896	16						
891.40	0.90	0.209	40						
902.91	0.40	0.732	16						
911.96	0.42	0.352	20						
924.40	0.43	0.590	18						
941.23	0.44	0.722	15						
954.16	0.67	0.597	16						
969.90	0.68	0.663	20						
979.39	0.80	1.18	16						
988.56	0.90	0.371	30						
1023.76	0.90	0.565	30						
1041.34	0.90	0.714	25						

[a] Energy taken from the level scheme in Fig. 8.
[b] Sum of the L_2 and L_3 lines.
[c] The electron energy is calculated from the γ energy.
[d] Intensity of overlapping K, L, M, Auger lines have been subtracted from I_c.
[e] Intensity of overlapping K, L, M, Auger lines are included in the value of I_e.
[f] (I_e-L_2 83 Eu) means that the intensity of the L_2 electron conversion of the 83-keV line in ^{153}Eu has been removed from the value of I_e. (I_e-K166) means that the intensity of the K electron line of the 166-keV γ ray was

(*Continued*)

Conversion coefficients							
Experimental		Theoretical			Multipolarity	In-level	
I_e/I_γ	$\Delta(I_e/I_\gamma)/(I_e/I_\gamma)$	$E1$	$E2$	$M1$	of γ	scheme	Remarks
(11)	(12)	(13)	(14)	(15)	(16)	(17)	(18)
						√	
<0.009		0.0023	0.0060	0.0104	($E1$, $E2$)	√	
<0.008		0.0021	0.0054	0.0093	($E1$, $E2$)	√	
						√	
						√	
						√	
						√	
						√	

subtracted from I_e. Similarly the label ($I_e-L\cdots$) or ($I_e-M\cdots$) indicate the removal of the intensity of an L or M line.

[g] (I_e+M46) means that the intensity of the M electron conversion of the 46-keV γ in ^{152}Sm is included in the value of I_e. Similarly the notation ($I_e+K\cdots$) or ($I_e+L\cdots$) means that I_e includes a K or L line.

[h] Line used for energy calibration.

[i] Line may be shifted by an overlapping line.

[j] Intensity of similar energy line in Sm 150 was subtracted from I_e.

TABLE III. Bent-crystal gamma-ray data and magnetic-spectrometer conversion-electron data on the gamma transitions in ^{153}Eu following the β decay of ^{153}Sm. The format is the same as in Table II.

Bent-crystal spectrometer				Conversion-electron spectrometer						Conversion coefficients					Multipolarity
γ energy		γ intensity		γ energy	Assumed	Electron energy		Electron intensity		Experimental		Theoretical			of γ rays
E_γ (keV)	ΔE_γ (keV)	I_γ (γ rays/100 captures)	$\Delta I_\gamma/I_\gamma$ (%)	E_γ (C.E.) (keV)	electron shell	E_e (keV)	ΔE_e (keV)	I_e (β rays/100 captures)	$\Delta I_e/I_e$ (%)	I_e/I_γ	$\Delta(I_e/I_\gamma)/I_e/I_\gamma$ (%)	$E1$	$E2$	$M1$	
(1)	(2)	(3)	(4)	(5)	(6)	(7)	(8)	(9)	(10)	(11)	(12)	(13)	(14)	(15)	(16)
69.675	0.005	5.82	7	69.70	K	21.19	0.03	21.9	20	3.74	21	0.626	2.82	4.44	$M1+$
					L_{I}	61.64	0.05	3.04	10	0.52	12	0.0609	0.231	0.590	(1.9 ± 0.2)% $E2$
					L_{II}	62.04	0.25	0.51	25	0.087	26	0.0166	2.38	0.0502	
					L_{III}	62.64	0.22	0.31	25	0.053	26	0.0218	2.69	0.0090	
					M	67.83	0.06	0.84	15	0.14	17				
					N	69.36	0.06	0.34	20	0.058	21				
75.42	0.01	0.209	5		K			0.075[a]	30	0.36	30	0.500	2.32	3.50	$E1$
83.37	0.01	0.237	5	83.40	L_{I}	75.35	0.2	0.08	30	0.34	30	0.0391	0.161	0.351	$M1+E2$
					L_{II}	75.68	0.2	0.17	30	0.71	30	0.0092	1.02	0.0293	
					L_{III}	76.47	0.2	0.14	30	0.59	30	0.0119	1.09	0.0053	
89.48	0.02	0.174	7		K			0.49[a]	20	2.82	20	0.320	1.52	2.15	$M1$
97.42	0.01	0.71	3		K			0.19[a]	20	0.27	20	0.256	1.22	1.68	$E1$
103.181	0.005	28.0[b]	3	103.17	K	54.65	0.05	40.3[b]	5	1.44	6	0.220	1.07	1.44	$M1+$
					L_{I}	95.11	0.05	5.40	5	0.19	6	0.0228	0.0984	0.191	(1.0 ± 0.2)% $E2$
					L_{II}	95.54	0.2	0.55	15	0.020	15	0.0045	0.378	0.0156	
					L_{III}	96.25	0.25	0.18	30	0.0064	30	0.0057	0.381	0.0028	
					M	101.60	0.3	1.42	5	0.051	6				
					N	103.07	0.3	0.41	7	0.015	8				
172.85	0.02	0.064	8	172.81	K	124.29	0.2	0.03	30	0.47		0.0553	0.238	0.336	$M1$
411.68	0.20	0.002	40												
494.08	0.25	0.004	20												
521.30	0.30	0.006	20												
531.66	0.30	0.042	8												
538.66	0.30	0.015	15												
596.85	0.30	0.006	20												
609.34	0.30	0.010	15												

[a] Intensity taken from Ref. 24.

[b] Line used for intensity calibration.

the errors quoted for otherwise similar lines in the table.

In the computer analysis of the data, each line was approximated with a Gaussian curve when well-resolved regions of the spectrum were fitted. The actual line shape follows the Gaussian shape to within a few percent, with most of the differences in the wings. When the complex doublet and triplet structures were fitted, a more elaborate line shape was used for each diffraction peak which followed the actual line shape to within a few tenths of a percent.

The γ-ray energies in column 1 of Table II are based on the previously established energy calibration of the bent-crystal spectrometer and were checked in this experiment by comparing the energies obtained for some of the strong lines in the ^{149}Sm$(n,\gamma)^{150}$Sm spectrum with the published values[20,23,24] for these lines.

The calibration of the low-energy end of the spectrum was checked by comparing the energies observed for the Sm x rays with the published values of Bearden,[25] which are based on the tungsten $K-L_{III}$ x ray as a primary standard. All calibrations agreed to within 1 part in 10^4.

The main difficulty in the analysis of the data came in the energy region above 400 keV, where the energy spacing between lines became of the same order of magnitude as the linewidth. The larger errors quoted for many of the lines above 400 keV reflect resolution problems rather than poor counting statistics. The errors given for the γ-ray energies in column 2 of Table II are probable errors and do not include a possible systematic error that might be present in all the numbers, which could be as large as 1 part in 10^4. The γ intensities were normalized by comparing them with the strength of the strong line at 103 keV in the ^{153}Eu spectrum emitted after the β decay of ^{153}Sm. On the basis of previously published studies[26] of this decay, the ^{153}Eu line was assumed to have an intensity of 28 γ rays per 100 neutron captures in ^{152}Sm when the β-decay rate was in equilibrium with the neutron-capture rate. The errors quoted on the γ intensities are probable errors and reflect only errors in the relative efficiency of the bent-crystal spectrometer and in the counting statistics of the data; they do not include any systematic error that might be present in the assumed value[26] for the 103-keV line in ^{153}Eu. Table III lists the precision energies and intensities of the other 24 lines in the bent-crystal gamma spectrum that are associated with the β decay of ^{153}Sm, the identification being made by observing the 47-h decay in their intensities during a period in which the pile was shut down.

As mentioned above, the ^{152}Sm$(n,\gamma)^{153}$Sm spectrum was complicated by the presence of gammas from the ^{149}Sm$(n,\gamma)^{150}$Sm, ^{150}Sm$(n,\gamma)^{151}$Sm, ^{151}Sm$(n,\gamma)^{152}$Sm, and ^{154}Sm$(n,\gamma)^{155}$Sm reactions, which were identified and removed from the list by means of comparison with the runs obtained with samples having other isotopic enrichments. There were also transitions produced by the ^{153}Sm$(n,\gamma)^{154}$Sm, and ^{153}Eu$(n,\gamma)^{154}$Eu reactions. They were identified by observing the variations in their intensities as a function of time. The ^{153}Sm$(n,\gamma)^{154}$Sm γ rays varied in exactly the same manner as the 103-keV gamma associated with the β decay of ^{153}Sm, while the ^{153}Eu$(n,\gamma)^{154}$Eu gammas showed a linear increase in their intensity as a function of integrated neutron flux. There are still about 40–60 weak γ rays in the spectrum (but not listed in Table II) whose isotopic identity has not been established. It is possible that more analysis (e.g., multiple sums early and late in the experiment, or new experiments with other isotopes) will lead to their identification, but this has not yet been done.

B. Conversion-Electron Measurements

The conversion-electron spectrum of transitions in ^{153}Sm following neutron capture in ^{152}Sm was measured with the high-resolution magnetic β-ray spectrometer at the research reactor of the Technische Hochschule München.[23,27,28] The results of these measurements appear in columns 5–10 of Table II along with the bent-crystal data. Electron counting rates were measured at 3500 steps in the magnetic field to cover the electron-energy range from 0 to 650 keV. Three separate runs were made. The counting period for each step was 1 min for one run and 4 min for each of the other two runs. The lines of ^{153}Eu following the β decay of ^{153}Sm were also measured when the reactor was shut down. Their energies and intensities are presented in columns 7 and 9 of Table III, which also includes the corresponding bent-crystal data. The capturing sample in the conversion-electron work measured 10×80 mm and consisted of 0.5 mg/cm^2 of samarium metal enriched to 87.4% in ^{152}Sm. The abundances of the other isotopes were 0.53% ^{144}Sm, 3.11% ^{147}Sm, 2.39% ^{148}Sm, 2.71% ^{149}Sm, 1.39% ^{150}Sm, and 2.48% ^{154}Sm. The samarium sample, which was obtained as an oxide, was first reduced to the pure metal and then evaporated on an Al-foil backing 0.2 mg/cm^2 thick. The resolution with this arrangement was $\Delta(B\rho)/B\rho=0.43\%$ at 95 keV and $\Delta(B\rho)/B\rho=0.28\%$ at 230 keV. The electrons were detected by a proportional counter with a 50-μg/cm^2 Formvar window.[29] The low-energy part of the spectrum was measured with the target maintained at 12 keV to preaccelerate the electrons. The neutron flux at the target was 1.5×10^{12} neutrons/cm^2 sec.

[23] E. Bieber, T. v. Egidy, and O. W. B. Schult, Z. Physik **170**, 465 (1962).
[24] O. W. B. Schult, Z. Naturforsch. **16A**, 927 (1961).
[25] J. A. Bearden, *X Ray Wavelengths* (U.S.A.E.C. Division of Technical Information Extension, Oak Ridge, Tenn., 1964).
[26] *Nuclear Data Sheets*, compiled by K. Way *et al.* (Printing and Publishing Office, National Academy of Science—National Research Council, Washington 25, D. C., 1963), 5-5-34.
[27] T. v. Egidy, Ann. Physik **9**, 221 (1962).
[28] E. Bieber, Z. Physik **189**, 217 (1966).
[29] T. v. Egidy, E. Bieber, and Th. W. Elze, Z. Physik **195**, 489 (1966).

A part of the measured electron spectrum is shown in Fig. 3(a). Below it [Fig. 3(b)] is the same region of the spectrum as seen with the bent-crystal spectrometer. The notations $K269$ and $K276$ are used in Fig. 3(a) to indicate the K conversion lines of the 269- and 276-keV γ rays from the ^{152}Sm$(n,\gamma)^{153}$Sm reaction. The $K272$ ^{150}Sm notation indicates the position of a similar line from the ^{149}Sm$(n,\gamma)^{150}$Sm reaction. The lines in the bent-crystal data [Fig. 3(b)] associated with the ^{153}Sm level scheme are labeled with their measured gamma energies. The ^{154}Eu and (Eu) labels indicate lines associated with europium level schemes. Note that the line ($K272$) identified with the ^{149}Sm$(n,\gamma)^{150}$Sm spectrum is much weaker relative to the ^{152}Sm$(n,\gamma)^{153}$Sm lines in the bent-crystal measurements than in the conversion-electron work. This is a direct result of the much larger percentage of ^{149}Sm in the conversion-electron source than in the bent-crystal sample; this difference is somewhat enhanced because some conversion of ^{149}Sm atoms to ^{150}Sm atoms through neutron capture has taken place in the bent-crystal sample. The electron lines were fitted with a theoretical line shape that was varied with energy by means of a computer program.[30] This program computed the relative intensities of the lines and their positions on a scale that is linearly related to their $\beta\rho$ values. The electron energies calculated from these values were calibrated with the ^{153}Sm lines at 119.770, 127.300, 175.365, and 182.901 keV, the 103.181-keV line[24] from ^{153}Eu, and the 333.945-, 439.398-, and 505.400-keV lines[23] from ^{150}Sm. These previously published values agree with the ^{153}Sm bent-crystal results of this paper and with the previously published results of Smither[20] to within a few hundredths of a keV, so no renormalization was needed when the conversion-electron data were combined with the bent-crystal data in Table II.

The relative electron intensities from the different runs were corrected for absorption in the counter window and averaged. The intensities were then calibrated with the observed intensity (corrected for activation) of the K conversion of the 103-keV line of ^{153}Eu. The gamma intensity of this line was assumed to be 28.0 gammas per 100 decays of the ^{153}Sm ground state.[26] The relative intensities of the L-conversion lines confirm the $M1$ nature (99.0% $M1$+1.0±0.2% $E2$) of this transition and the corresponding theoretical conversion coefficient was used to obtain the absolute conversion-electron intensity of the 103-keV line. The present analysis of $M1+E2$ mixing ratios is in good agreement with those reported by Suter *et al.*[31] Thirty-five of the lines in the electron spectrum were identified with neutron capture in ^{149}Sm by comparing our results with those of Elze[32] and these have been omitted from Table II. Our conversion-electron energies and intensities are in good agreement with those of Prokofiev *et al.*[33]

C. K- and L-Conversion Coefficients

The K and L coefficients obtained by combining the bent-crystal and conversion-electron data appear in column 11 of Tables II and III under the heading I_e/I_γ. These results were compared with the theoretical conversion coefficients for $E1$, $E2$, and $M1$ multipolarities which are given in columns 13–15, respectively, and the inferred multipole assignment appears in column 16. The theoretical values were obtained for each line through a computer program which makes a linear interpolation on a log-log plot between the calculated values of Sliv and Band.[34] Possible admixtures of $M2$ and higher multipoles were not considered. The errors

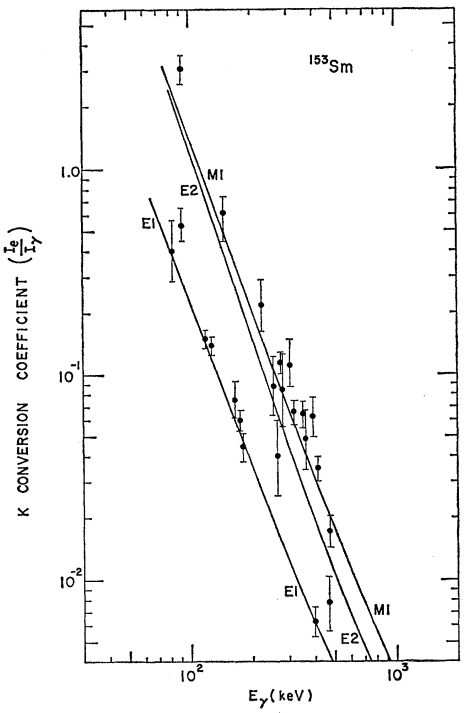

FIG. 4. A log-log plot of the experimental K conversion coefficients for the ^{153}Sm γ-ray spectrum. The solid lines indicate the theoretical values for the $E1$, $M1$, and $E2$ multipoles.

[30] T. v. Egidy and Th. W. Elze, FRM-Bericht Nr. 79, Technische, Hochschule München, 1966 (unpublished).

[31] T. Suter, P. Reyes-Suter, S. Gustafsson, and I. Markland, Nucl. Phys. **29**, 33 (1962).

[32] Th. W. Elze, Z. Physik **194**, 280 (1966).

[33] P. T. Prokof'ev, M. K. Balodis, Ya. Ya. Bersin, V. A. Bondarenko, N. D. Kramer, E. Ya. Lure, G. L. Rezvaya, and L. J. Simonova, *Atlas of Conversion Electron Spectra following Thermal Neutron Capture of Nuclei with $A=143$ to $A=197$ and Level Schemes* (Izdated'stvo "Zinatne," Riga, 1967).

[34] L. A. Sliv and I. M. Band, in *Alpha-, Beta-, and Gamma Ray Spectroscopy*, edited by K. Siegbahn (North-Holland Publishing Co., Amsterdam, 1965), Vol. II, p. 1533; L. A. Sliv and I. M. Band, *Coefficients of Internal Conversion of Gamma Radiation* (Academy of Sciences of U.S.S.R., Moscow and Leningrad, 1956), Parts I and II [issued in U.S.A. as Report No. 571CCK1, Physics Department, University of Illinois, Urbana, Ill. (unpublished)].

TABLE IV. Ge-diode data on the high-energy gammas from $Sm^{152}(n, \gamma)Sm^{153}$. The γ energies and intensities are given in columns 1 and 3. The errors quoted are the probable errors of the values with reference to the strong line at 5741.97 keV (see text for limits on the absolute errors). Column 5 gives the excitation energy of the level fed by the γ ray, as derived from the γ energies. Columns 7 and 8 give the corresponding level energies and the spins and parities as given in the final level scheme. Column 9 gives the inferred multipolarity of the γ ray.

High-energy γ rays (Ge diode data)				Inferred level energy		Corresponding values from level scheme		Inferred multipole for high energy γ	Remarks
E_γ (keV)	ΔE_γ (keV)	I_γ (γ's/100 captures)	$\Delta I_\gamma/I_\gamma$ (%)	E_f (keV)	ΔE_f (keV)	E_f (keV)	J^π		
(1)	(2)	(3)	(4)	(5)	(6)	(7)	(8)	(9)	(10)
5869.20	±0.10	0.142	6	0.00		0.0	$\frac{3}{2}^+$	$M1$	
5862.1	±0.4	0.014	30	7.2	±0.4	7.535	$\frac{5}{2}^+$	$E2$, ($M1$)	
5833.47	0.10	1.09	4	35.82	0.10	35.843	$\frac{3}{2}^-$	$E1$	
(5815.7)[a]		≤0.004				53.533	$\frac{7}{2}^+$, ($\frac{5}{2}^+$)	($E2$, $M3$)	
(5803.8)		≤0.004				65.475	$\frac{9}{2}^+$, $\frac{7}{2}^+$, $\frac{5}{2}^+$		
(5778.4)		≤0.004				90.874	$\frac{5}{2}^-$	($M2$)	
(5756.3)		≤0.004				112.954	$\frac{9}{2}^+$, $\frac{9}{2}^\pm$, $\frac{5}{2}^\pm$		
5741.97	0.10	4.35	4	127.32	0.10	127.298	$\frac{3}{2}^-$	$E1$	
(5675.1)		≤0.004				174.17	$\frac{7}{2}^-$	($E3$)	
(5686.4)		≤0.008				182.90	$\frac{5}{2}^-$	($M2$)	Complicated by the presence of a single-escape peak
(5674.6)		≤0.003				(194.65)	($\frac{5}{2}^\pm$, $\frac{7}{2}^+$)		
(5607.0)		≤0.003				262.33	$\frac{7}{2}^+$, ($\frac{5}{2}^+$)	($E2$, $M3$)	
(5603.4)		≤0.014				(265.93)	($\frac{7}{2}^-$, $\frac{5}{2}^\pm$)		
5592.48	0.12	0.085	10	276.81	0.12	276.71	$\frac{3}{2}^+$	$M1$	
5548.12	0.12	0.120	7	321.19	0.12	321.11	$\frac{3}{2}^+$	$M1$	
5513.8	±0.7	0.007	40	355.5	0.7	356.69	$\frac{5}{2}^+$	$E2$, ($M1$)	
5507.4	±0.5	0.010	30	361.9	±0.5	362.29	$\frac{5}{2}^+$	$E2$, ($M1$)	
(5498.1)		≤0.003				(371.04)	($\frac{9}{2}^-$, $\frac{7}{2}^-$)		
5463.9	0.2	0.33	6	405.4	0.2	405.46	$\frac{3}{2}^-$	$E1$	
5454.3	0.2	0.24	8	415.0	0.2	414.91	$\frac{1}{2}^+$, $\frac{3}{2}^+$	$M1$	
(5422.1)		≥0.003				447.07	$\frac{5}{2}$, $\frac{7}{2}$	($E2$, $M2$)	
(5125.1)		≤0.003				450.04	$\frac{5}{2}^-$	($M2$)	
5388.10	±0.16	0.41	6	481.19	0.16	481.08	$\frac{3}{2}^+$	$M1$	
(5368)		≤0.01				(501)[b]	≥$\frac{5}{2}$		
(5347.7)		≤0.01				524.36	$\frac{5}{2}$		
5239.2	±0.2	1.08	6	630.1	0.2	629.90	$\frac{3}{2}^-$	$E1$	
5174.0	±0.3	0.61	6	695.3	0.3	695.83	$\frac{1}{2}^{(+)}$, $\frac{3}{2}^{(+)}$		
(5132.4)		≤0.04				734.90	$\frac{5}{2}$		Complicated by Sm^{150} line
5119.2	0.5	0.40	8	750.1	0.5	750.32	$\frac{1}{2}$, $\frac{3}{2}$		
4947.2	0.5	0.16	10	930.5	0.5		$\frac{1}{2}$, $\frac{3}{2}$		Possible doublet
4865.0	0.5	0.37	8	984.3	0.5		$\frac{3}{2}$		Doublet
4851.0	0.6	0.09	25	1015.0	0.6				Doublet
4758.9	0.6	0.11	25	1110.4	0.6		$\frac{3}{2}$		
4698.6	0.5	0.96	7	1107.6	0.5		$\frac{1}{2}$, $\frac{3}{2}$		
4646.5	0.7	0.14	15	1222.8	0.7		$\frac{1}{2}$, $\frac{3}{2}$		
4546.6	0.6	0.84	7	1322.7	0.6		$\frac{1}{2}$, $\frac{3}{2}$		
4525.6	0.7	0.26	10	1343.8	0.7		$\frac{1}{2}$, $\frac{3}{2}$		
4506.5	0.6	0.67	8	1362.8	0.6		$\frac{1}{2}$, $\frac{3}{2}$		

[a] The parentheses around E_γ indicate that the value comes from the level scheme.

[b] The parentheses around E_L indicate that the value of the level energy comes from the (d, p) work of Ref. 7.

on the conversion coefficients vary from a few percent for the strong lines to 50–60% for the weak ones. In most cases it is possible to choose between an $E1$ assignment and an $E2$ or $M1$ assignment; and although the conversion coefficients usually are not accurate enough to calculate a meaningful $E2+M1$ admixture, they are often sufficiently accurate to suggest the main component in these transitions. Thus the label $M1$ in column 16 of Tables II and III means "mostly $M1$" and similarly for the notation $E2$, etc. It should be

remembered, however, that multipole assignments based only on K-conversion coefficients are not unique; the value of an $M1$ multipole can be reproduced by a combination of $E2+E0$ multipoles. It is also possible to confuse the value obtained for a close doublet consisting of two $E2$ transitions with that appropriate for a similar close doublet made up of an $E1$ and an $M1$ transition, as appears to be the case for the possible doublet at 470 keV. For a few of the low-energy transitions it is possible to calculate the $E2+M1$ admixtures from the conversion-electron intensities of the L subshells. These admixtures are noted in the multipole column as $M1+(20\pm15)\%E2$, which means $(80\pm15)\%$ $M1+(20\pm15)\%$ $E2$. In Fig. 4, a log-log plot of the observed K-conversion coefficients, it can be seen that the $E1$ values appear to be 5–10% too high. This suggests a 5–10% systematic error in all of the values. A 5–10% reduction of all experimental values improves the fit between the $M1$ and $E2$ theoretical values (solid lines) and the measured $M1+E2$ admixture as well, most of these values falling close to the $M1$ theoretical curve.

D. High-Energy Ge-Diode Data

The high-energy (4–6 MeV) portion of the (n,γ) spectrum was measured with a Ge(Li) detector used in conjunction with an in-pile sample facility (3×10^{13} neutrons/cm^2 sec at sample position) at the Argonne research reactor CP-5. A series of runs was made with three neutron-capturing samples, each enriched in a different isotope of samarium—the first to 81% ^{149}Sm, the second to 97% ^{150}Sm, and the third to 99% ^{152}Sm. A comparison of the relative intensities of the γ-ray lines in the spectra obtained with these samples led to the identification of 23 transitions in the ^{152}Sm$(n,\gamma)^{153}$Sm spectrum with energies between 4.5 and 5.9 MeV. The energies E_γ and intensities I_γ of these lines are given in Table IV, which also lists (column 5) the energy E_L of the level suggested by each γ ray on the assumption that the γ ray is a direct transition from the neutron-capture state. The level energy is then $E_L=5869.29$ keV$-E_\gamma$, the 5869.29 keV being the energy of the ground-state transition. For ease in comparison, column 7 gives the level energies deduced from the precision energy values of the low-energy γ's and column 8 lists the appropriate spin and parity assignment for each level. Column 9 gives the multipolarity of the high-energy γ ray as inferred from these spin and parity assignments. The errors quoted on the γ energies reflect only the errors associated with the location of the centroid of the peak and the calibration of the energy per channel for a limited region (4–6 MeV) of the spectrum. These are therefore the errors on the energy differences between the 5869.29-keV ground-state transition and the γ transitions in question.

The experimental data on the ^{152}Sm$(n,\gamma)^{153}$Sm spectrum consisted of 14 separate runs taken during two different running periods. A new sample in a new source holder was used in the second running period, but both samples came from the same batch of separated isotopes as was used in the bent-crystal experiment; the relative isotopic abundances are listed in Table I. The high enrichment of ^{152}Sm (99.06%) as compared with the small percentage of ^{149}Sm (0.11%) was very important in this experiment, because some of the lines in the ^{149}Sm$(n,\gamma)^{150}$Sm fall very close in energy to lines in the ^{152}Sm$(n,\gamma)^{153}$Sm spectrum. The first sample consisted of 85 mg of Sm_2O_3 in a carbon source holder. The measurements on each sample included both runs in which the full spectrum was recorded in the 4000-channel pulse-height analyzer with an energy scale of $\sim$2.5 keV per channel and runs in which the 4–8-MeV portion of the spectrum was expanded to $\sim$0.9-keV per channel through the use of a biased amplifier. Data runs were also made with a coincidence gate that recorded the spectrum in the Ge(Li) detector only when two coincident annihilation gammas escaped from this detector and were detected in NaI crystals placed on opposite sides of it. These runs were used to help identify double-escape peaks in the spectrum.

The position of the sample in the reactor was varied in different runs in order to change the neutron flux at the sample as well as the distance between sample and detector. This procedure helped to distinguish between γ transitions associated with neutron capture in the sample and transitions associated with background sources. This change in sample position was also used to vary the counting rate in the Ge(Li) detector. The amount of polyethene absorber placed between the in-pile source and the detector was also varied to control the counting rate and to change (and thereby identify) any background lines associated with fast neutrons scattered by the sample. The use of the same sample holder with samples of different isotopic abundance as well as the above-mentioned changes in experimental conditions allowed one to eliminate γ-ray lines coming from sources other than the Sm_2O_3 sample, and made it possible to assign a number of weak lines in the γ spectrum to the ^{152}Sm$(n,\gamma)^{153}$Sm reaction.

The γ energies and intensities in Table IV come from a detailed analysis of one of the biased-amplifier runs in which the energy scale was expanded to $\sim$0.88 keV per channel. A small section of this run, showing the transition to the ground state and the first few excited states, appears in Fig. 5. The expanded view shows the very weak transition ($I_\gamma=0.014\%$) to the 7.53-keV first excited state. The linewidth [full width at half maximum (FWHM)] in this energy region was 6.5 keV. The calibration (keV per channel) was made by comparing the channel spacings between the ground-state transition and transitions to the 35-, the 127-, and the 481-keV levels and adjusting the energy difference per channel until these spacings were most nearly equal to the level spacings based on the bent-crystal-spectrometer data. Although this procedure introduces some systematic error (1 part in 10^4) in the absolute energy

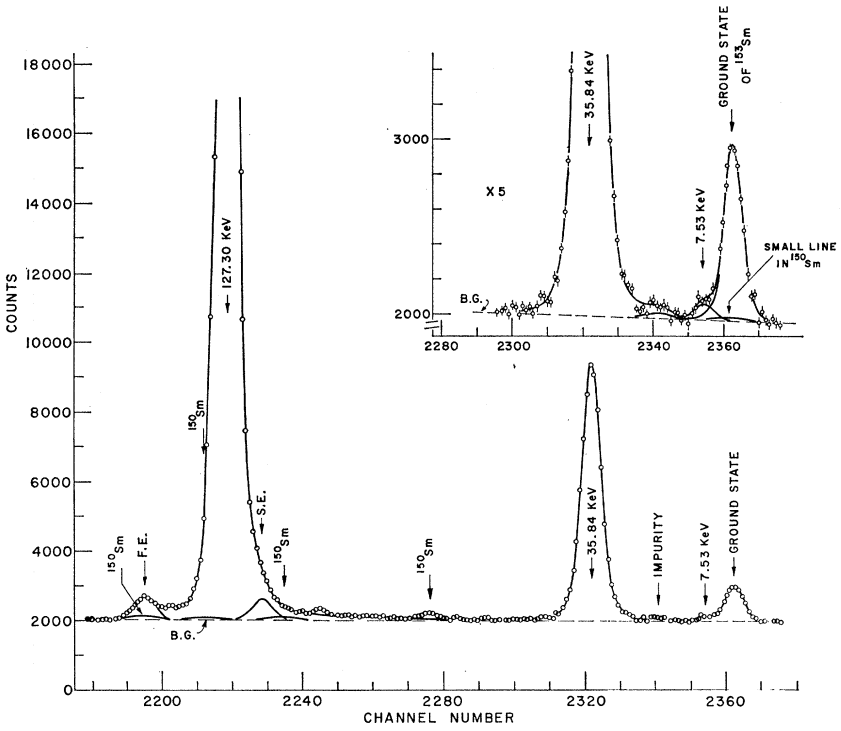

FIG. 5. Part of the high-energy spectrum of ^{152}Sm (n, γ) ^{153}Sm as seen with the Ge(Li) detector used in conjunction with a 4000-channel analyzer. The double-escape peaks associated with the ^{152}Sm (n, γ) ^{153}Sm reaction are labeled with the energy of the level at which they terminate in the ^{153}Sm level scheme. The notations FE and SE indicate full-energy and single-escape peaks from the same reaction. The ^{150}Sm label indicates lines from the ^{149}Sm (n, γ) ^{150}Sm reaction. The insert shows the resolution of the very weak transition ($I_\gamma = 0.014$ γ rays per 100 neutron captures) to the 7.53-keV first excited state.

spacings, it eliminates any systematic differences between the energy calibrations of the low-energy bent-crystal data and those of the Ge-diode data. This is a very useful procedure because it allows one to predict the position of a new level to within a few tenths of a keV and thus to predict the energies of the associated γ transitions with similar error without worrying about absolute energies or absolute energy differences. This strongly reduces the probability of assigning the wrong combination of γ transitions (an accidental fit of γ's to an energy near that of the level energy) to a level suggested by a high-energy γ transition.

The absolute values of the γ energies were obtained by measuring the relative energies of the stronger lines in carbon and nitrogen and adjusting this set of values for the best fit with the published values.[35] The errors on the absolute γ-ray energies E_γ are ± 2 keV. The γ energies were originally calibrated with the values of Elze[32] for the ^{149}Sm(n, γ)^{150}Sm spectrum. A recalibration of this spectrum in terms of the carbon and nitrogen lines leads to a binding energy of ^{150}Sm which is 4 keV higher than that obtained by Elze.[32] The ^{152}Sm(n, γ)^{153}Sm γ energies are increased by 6 keV. This change in the method of calibration accounts for the difference between the values given in Table IV and those given in a preliminary report.[14]

The relative intensities of the high-energy gammas were obtained from Ge-diode data by use of the calibration curve of Thomas *et al.*[35] The absolute intensities were obtained by comparing the relative γ intensities in the ^{152}Sm(n, γ)^{153}Sm spectrum with those observed in the ^{149}Sm(n, γ)^{150}Sm spectrum and normalizing these so that they agreed with the previously published values of Groshev *et al.*[36] The isotopic abundance of ^{149}Sm in the sample was checked by comparing the intensities of the strong lines of the ^{149}Sm(n, γ)^{150}Sm spectrum in the bent-crystal data with those in the ^{152}Sm(n, γ)^{153}Sm spectrum. On the basis of this approach, the isotopic abundance of ^{149}Sm in the sample was found to be $(0.095 \pm 0.010)\%$, which is in good agreement with the value $(0.11 \pm 0.02)\%$ quoted by the supplier.[19] The 10% uncertainty in the ^{149}Sm abundance introduces an additional 10% uncertainty into this calculation of absolute intensity and, when added to the error of 20% quoted by Groshev *et al.*,[36] leads to an uncertainty of 25% in the absolute intensity. The errors quoted on the γ intensities in Table IV are errors on the relative intensities only and do not include the above-mentioned possible systematic error of 25% in their absolute values.

E. β Decay of ^{153}Pm

Ge(Li) and Si(Li) detectors were used to investigate the γ-ray spectrum associated with the 5.5-min β decay from ^{153}Pm to ^{153}Sm. The ^{153}Pm source was made by placing 90 mg of highly enriched ^{154}Sm metal in the

[35] G. E. Thomas, D. E. Blatchley, and L. M. Bollinger, Nucl. Instr. Methods **56**, 325 (1967).

[36] L. V. Groshev, A. M. Demidov, V. A. Ivanov, N. V. Lutsenko, and V. I. Pelekhov, Nucl. Phys. **43**, 669 (1963).

TABLE V. Experimental data associated with the β decay of ^{153}Pm to ^{153}Sm. The first three columns give the energy E_i of the level in ^{153}Sm being fed, the relative intensity I_β of the β-decay branch to this level, and the corresponding logft value. E_γ and I_γ are the γ energy and γ intensity, respectively, as measured with the Ge(Li) detector. I_β(rel) is the relative intensity of the γ-ray transitions when normalized so that the transition to the ground state is 100. The I_γ(rel) based on the β-decay data is compared with the I_γ(rel) values taken from the (n, γ) data in Table II. E_f is the energy of the final state of the γ transition. All energies are based on the Ge(Li) detector work. Intensity errors are given in parentheses following the number.

(1) E_i (keV)	(2) I_β(rel) (%)	(3) logft	(4) E_γ (keV)	(4) ΔE_γ (keV)	(5) I_γ (γ's per 1000 β's)	(6) I_γ(rel) of β-decay data	(7) I_γ(rel) of (n, γ) data	(8) E_f (keV)
35.9	55	5.4	35.9±0.2		~250	100	100	0.0
			28.3	0.2	~80	~30	34(5)	7.6
91.9	3	6.7	91.0[a]	0.3	35[a](9)[b]	100	100	0.0
			83.3	0.5	11(3)	33(7)	33(5)	7.7
127.3	34	5.6	127.3	0.3	140[b]	100	100	0.0
			119.5	0.3	60(6)	43(4)	43(3)	7.8
183.0	8	6.2	183.0	0.5	27(3)	100	100	0.0
			175.3	0.5	20(3)	75(8)	81(6)	7.7
			147.3	0.5	5(1)	19(4)	16(2)	35.7
			129.3	0.5	18(5)	56(10)	46(3)	53.7

[a] This line consists of three different transitions as indicated in the (n, γ) work. This complication has been taken into account in calculating the logft values.

[b] The errors in parentheses reflect only the error in the intensity relative to that of the 127.3-keV line; they do not include the uncertainty in the absolute intensity of this reference line.

bremsstrahlung flux generated by 50-MeV electrons from the linear accelerator in Darmstadt. The bremsstrahlung radiation converted some of the ^{154}Sm to ^{153}Pm through the ^{154}Sm$(\gamma, p)^{153}$Pm reaction.

Each experimental cycle consisted of a 7-min irradiation period followed by a 1–2-min waiting period to reduce short-lived activities. During the waiting period the sample was transported from the accelerator to the laboratory through a pneumatic tube.

In order to identify the ^{153}Pm gamma lines by their half-lives, the pulse-height spectrum of the sample was measured with a 2.8-cm^3 Ge(Li) detector in 8 time periods of 5 min each. The spectrum of each time period was stored in a separate group of 512 channels in the analyzer. The sample was then returned to the accelerator facility for reirradiation and the cycle was repeated until good statistics were obtained in all spectra. Seven γ lines were found with the half-life of ^{153}Pm. The decay of the intensity of the strong line at 127.3 keV, shown in Fig. 6, corresponds to a half-line of 5.3± 0.3 min.

Because of the insufficient energy resolution of the 2.8-cm^3 Ge(Li) detector used in the initial runs, one additional run was made with a 3.5-cm^3 high-resolution (1.4 keV FWHM at 127 keV) detector. The pulse-height spectrum was spread over 1024 channels, and four 8-min runs taken sequentially were stored in separate sections of the analyzer. The spectrum shown in Fig. 7 was obtained by subtracting the spectrum of the third counting period from that of the first counting period (which started 2 min after irradiation) in order to eliminate the long-lived background of ^{153}Sm, etc. The insert shows a part of the low-energy spectrum of the sample, measured with a thin-window Si(Li) detector. The time sequence and the background reduction of this run were similar to those used in obtaining Fig. 7.

In all spectra, ten γ lines were identified with the β decay of ^{153}Pm to ^{153}Sm through the constant ratio of their intensities to that of the strong 127.3-keV line during the counting period. Their energies and relative intensities are given in Table V. The absorption of the 28.3- and 35.9-keV γ rays in the powdered Sm metal target and in the detector windows prevented a reliable quotation of their intensities relative to that of the 127.3-keV line. Because tantalum was introduced into the

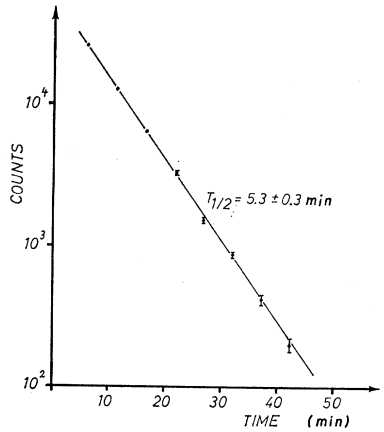

FIG. 6. The decay of the intensity of the strong 127.3-keV ^{153}Sm line exited in the β decay of ^{153}Pm. The 7-min irradiation producing the ^{153}Pm source ended at zero time on the horizontal scale.

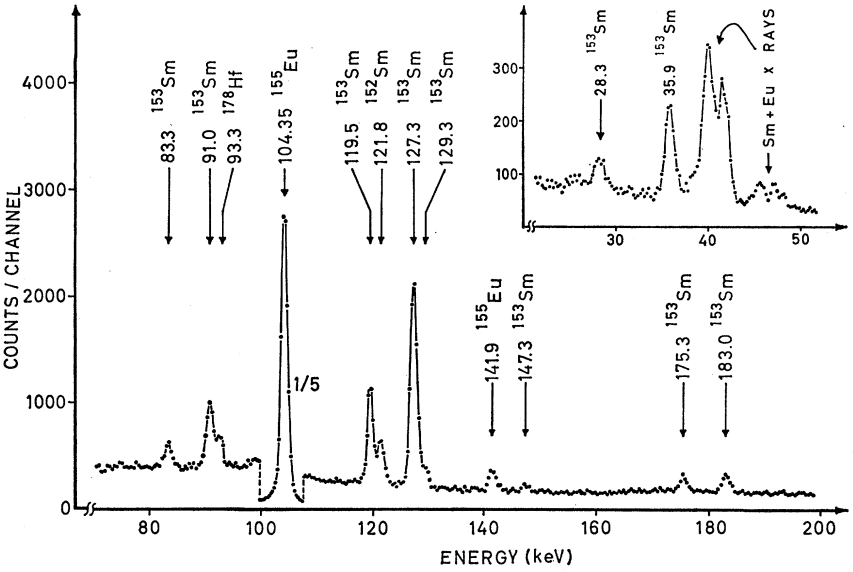

FIG. 7. The Ge(Li) pulse-height spectrum obtained in the interval 2–10 min after irradiation of ^{154}Sm to produce ^{153}Pm, after the spectrum taken in the 18–26 min interval following irradiation has been subtracted from it to remove background lines. The lines labeled ^{153}Sm are ^{153}Sm lines associated with the β decay of ^{153}Pm; similarly the lines labeled ^{153}Eu, ^{178}Hf, and ^{152}Sm are transitions in these nuclides.

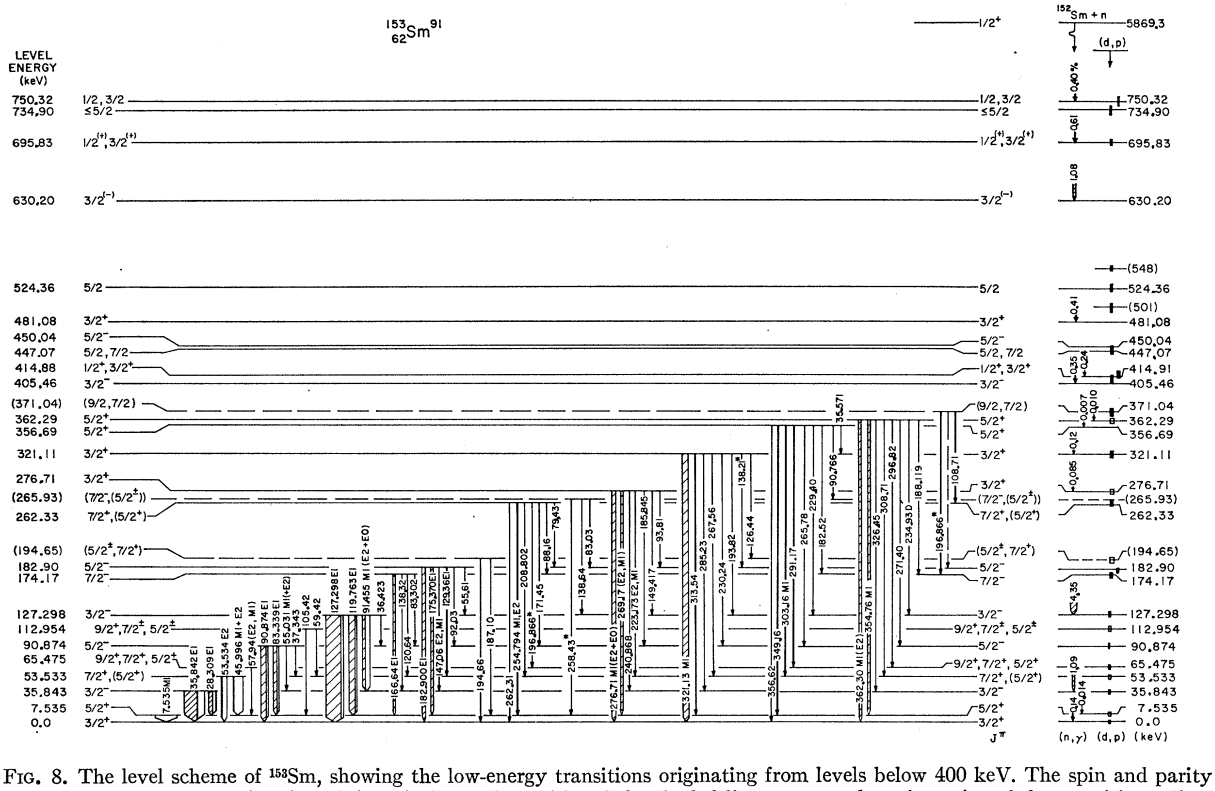

FIG. 8. The level scheme of ^{153}Sm, showing the low-energy transitions originating from levels below 400 keV. The spin and parity assignments come from the (n, γ) and (n, e^-) data. The widths of the shaded lines suggest the γ intensity of the transition. When the conversion-electron intensity is appreciable, it appears as an unshaded portion of the line. The labels on the transitions give their energies (in keV) and multipole assignments. The vertical arrows on the right-hand side of the level scheme indicate the presence of direct (n, γ) transitions from the neutron-capture state. The energy levels from the early (d, p) work of Kenefick and Sheline (Ref. 7) appear on the right-hand side of the level scheme as solid bars whose vertical heights reflect the uncertainty in their energies. The open bars correspond to the levels added in the recent (d, p) and (d, t) work (Ref. 15). The spin and parity assignments are repeated on the right-hand side of the level scheme. The parentheses around some of the level energies reflect some uncertainty in the method used to determine them.

sample during its conversion from Sm_2O_3 to metallic form, one line at 93.3 keV is associated with the β decay of 9.5-min ^{178}Ta. The background lines at 104.3 and 141.0 keV belong to ^{155}Sm, which is created by neutron capture in ^{154}Sm. A 121.8-keV line is emitted from ^{152}Sm formed in the β decay of ^{152}Pm (half-life = 6 min). This isotope is produced by the ^{154}Sm$(\gamma, np)^{152}$Pm reaction; which occurs with $\frac{1}{7}$ the frequency of the ^{154}Sm$(\gamma, p)^{153}$Pm reaction.[37] No other lines of ^{152}Sm were detected, nor does the well-known level scheme of ^{152}Sm lead one to expect any in the energy region investigated.

The ten lines of the ^{153}Pm decay were identified with ten transitions in the ^{152}Sm$(n, \gamma)^{153}$Sm spectrum, whose energies differ at most 0.4 keV from the ^{153}Pm data. These 10 transitions are associated with four initial states and decay to four final states in the proposed level scheme of ^{153}Sm discussed in Sec. III (see Fig. 8). The initial and final level energies, E_i and E_f, as calculated from the ^{153}Pm data, are given in Table V together with the relative intensities of the γ transitions. For ease of comparison, the appropriate relative intensities taken from the (n, γ) data are given in column 7 of Table V. Four pairs of the γ lines have an energy difference of about 7.5 keV, consistent with the assumption that each pair is composed of a transition to the ground state and to the proposed 7.53-keV state. The good agreement between the relative intensities of transitions assigned to the same initial state in the two reactions, constitutes an important check on the placement of these γ rays in the level scheme and on the existence of a 7.53-keV first excited state.

The relative intensities of the observed γ rays were used to calculate intensities for the β transitions. These intensities and the corresponding logft values are given in Table V. The work of Kotajima[38] presents no evidence for a strong β transition to the ground state; thus the correction to the above logft values for this additional β intensity cannot be too large. The moderate values of logft, which fall in the range 5.4–6.7, are consistent with the assignments for the four final states discussed in Secs. III, IV, and V.

F. 7.53-keV Transition in ^{153}Sm

Evidence for the 7.53-keV transition from the 7.53-keV level to the $\frac{3}{2}^+$ ground state was observed with a newly developed proportional counter[39,40] designed especially for low-energy γ rays. Two samples, one of natural Sm and one enriched in ^{153}Sm, were placed in an external neutron beam ($\sim 10^8$ neutrons/cm^2 sec) from the research reactor at Karlsruhe. A comparison of the two (n, γ) spectra allowed one to identify the contribution associated with the ^{152}Sm$(n, \gamma)^{153}$Sm reaction. The 7.5-keV γ was not observed directly. It was inferred[40] from the considerable excess of L x rays left over in the γ spectrum after accounting for the holes generated in the K and L shells from the electron conversion of the low-energy transitions of ^{153}Sm and ^{150}Sm (Table II and Ref. 32, respectively). The intensity of the excess L x rays indicate that the summed strength of the L_{II} and L_{III} conversion lines (L_I is not energetically possible) of the 7.5-keV transition is 50 ± 20 conversion electrons per 100 neutron captures. This is in good agreement with the deduced strong feeding of this level; the value calculated from the proposed level scheme is ≥ 34 transitions per 100 neutron captures. Since the total intensity of the 7.5-keV transition is less than 60 per 100 captures (based on the fact that the summed intensity of all other known ground-state transitions is >40 per 100 captures). This lower limit implies that the conversion is stronger in the L shell than in the M shell. A pure $M1$ transition would result in twice as much M-shell conversion than L-shell conversion and might appear to argue against an $M1$ assignment for this transition. However, a small admixture of $E2(\geq 0.1\%)$ is sufficient to account for the stronger L-shell contribution.

III. DEVELOPMENT OF LEVEL SCHEME

The (n, γ), (n, e^-), and β-decay data are combined with the results of the previously published (d, p) and (d, t) experiments[7,15] and β-decay work[38] to develop the level scheme of ^{153}Sm which is shown in Figs. 8 and 9. The level energies (in keV) are given on the left and are followed by the spin and parity assignments for the levels. These assignments are based only on the (n, γ) and conversion-electron data reported in this paper. The widths of the shaded arrows representing the gamma transitions are meant to suggest their relative intensities. When the conversion-electron intensity is appreciable, it appears as an unshaded portion of the line. The labels on the transitions give their energies (in keV) and multipole assignments when appropriate. The vertical arrows on the right-hand side of the level scheme indicate the presence of direct (n, γ) transitions from the neutron-capture state. The energy levels from the early (d, p) work of Kenefick and Sheline[7] appear on the right-hand side of the level scheme as solid bars whose vertical heights reflect the uncertainty in their energy measurements. The open bars correspond to the levels added in the recent (d, p) and (d, t) work.[13] The spin and parity assignments are repeated on the right-hand side of the level scheme. The parentheses around some of the level energies reflect some uncertainty in the method used to determine them, which usually means that there is no primary transition to this level and that relatively few γ transitions connect the level to the rest of the scheme. The parentheses around the second (or third) spin assignment means that the authors feel that this assignment is less probable than the preceding ones.

[37] K. Wien, Z. Physik **191**, 137 (1966).
[38] K. Kotajima, Nucl. Phys. **39**, 89 (1962).
[39] W. Kroy and T. v. Egidy, Nukleonik **8**, 435 (1866).
[40] M. Schön, Diplomarbeit, Physiks-Department, Technischen Hochschule München, 1969 (unpublished).

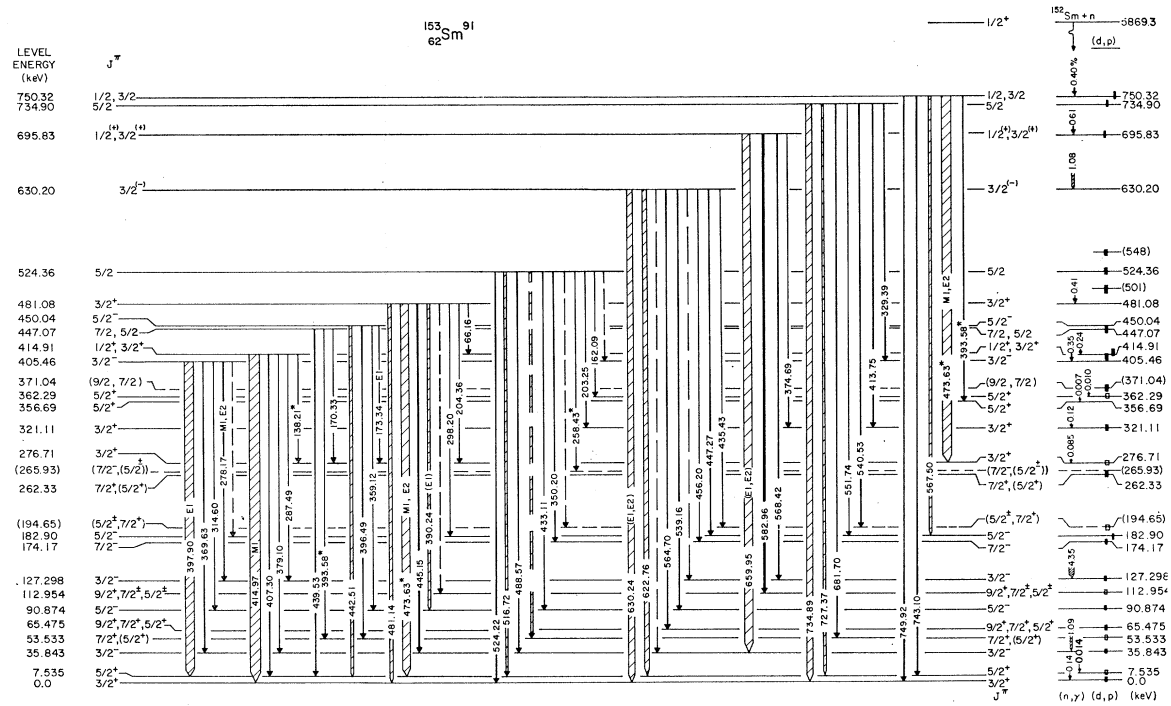

FIG. 9. The level scheme of ^{153}Sm, showing the γ transitions which originate from levels above 400 keV. The notation is the same as that in Fig. 8.

The level energies are based on the bent-crystal spectrometer work. As mentioned in Sec. II C, the intercalibration of the energy scales in the Ge-diode data and the bent-crystal spectrometer data made it possible to use the high-energy γ-ray data to infer the energy of a level to within a few tenths of a KeV in most cases. This considerably reduced the chance of assigning the wrong energy and wrong interconnecting γ rays to a new level on the basis of a chance agreement between different combinations of level energies and γ-ray energies. This is especially important for levels that are connected to the rest of the level scheme by only a few transitions.

The high precision of the γ-ray energies from the bent-crystal spectrometer measurements obviates most of the accidental fits, but there are many combinations of two γ rays whose energy difference matches one of the level differences in Fig. 9 to within their errors. The probability of finding one of these combinations in any 6-keV energy interval in which the (d, p) work suggests a level is also quite high. The probability that two such combinations in the 6-keV region would agree with each other within their errors (0.1–0.8 keV) and thus would suggest a possible level energy is low but not zero. Therefore, the reduction of the acceptable energy interval for the level from 6 keV (consistent with the accuracy of the (d, p) data to the 0.1 keV (appropriate for the high-energy (n, γ) data) results in a large reduction in the probability of making an error of this type. In two cases, the 501- and 548-keV levels, in which the (d, p) data suggest a level with $J \geq \frac{5}{2}$, considerable difficulty was experienced in choosing the γ transitions to connect this level to the rest of the level scheme. To avoid making the wrong choice between two or more possibilities, no selection was made and the level is indicated only by the (d, p) notation on the right-hand sides of Figs. 8 and 9.

The conversion-electron data (Sec. II B) were combined with the bent-crystal data to obtain K (and sometimes L) conversion coefficients and multipole assignments for most of the strong lines in the γ spectrum. These multipole assignments were used to determine the parity of 20 of the levels in Fig. 8 relative to the parity of the ground state, which was assumed to be a $\frac{3}{2}^+$ state.

Special efforts were made to detect all weak transitions that were not forbidden on the basis of our deduced spin and parity assignments, and to set upper limits on all of the missing transitions—even for $M2$, $E3$, and other transitions that are not expected to be seen. Table VI lists the upper limits on the intensities of some of these missing transitions. In many cases the upper limits are quite low (0.005% or less) and are therefore useful in developing the level scheme. Many of these upper limits were obtained by using a special automatic mode of operation of the bent-crystal spectrometer, in which the spectrometer repeatedly covered the same small region of the spectrum. By summing these runs, the number of counts often would be increased 20-fold and the sensitivity thereby increased by a factor of 4–5.

The spins and parities of the excited states were

TABLE VI. Upper limits on the γ intensities of missing transitions in the level scheme of ^{153}Sm. The γ-ray energies E_γ are taken from the differences $E_i - E_f$ between the initial and final energy levels in the level scheme. The transitions are listed in order of increasing E_i and secondarily by increasing E_f.

E_i (keV)	E_f (keV)	E_γ (keV)	I_γ (γ rays/100 captures)	Remarks
65.475	0.00	65.475	<0.003	
90.874	65.475	36.399	<0.010	
112.954	0.00	112.954	<0.003	
	35.843	77.111	<0.003	
	65.475	67.479	<0.003	
	90.874	22.080	<0.25	
	53.533	73.765	<0.0008	
	65.475	61.823	<0.004	
174.17	0.00	174.17	<0.001	
	65.475	98.695	<0.006	
	112.954	61.216	<0.0025	
	127.298	46.872	<0.002	Overlaps K-L_{III} x ray of Eu
182.90	65.475	117.42	<0.005	
	112.954	69.95	<0.005	
194.65	53.533	141.12	<0.006	
	65.475	129.17	<0.007	
	90.874	103.78	<0.003	
	112.95	81.70	<0.003	
	127.298	77.35	<0.004	
262.33	35.843	226.49	<0.003	
	112.954	149.38	<0.012	Under wing of 149.42 keV
262.33	127.298	135.03	<0.002	
	194.65	67.68	<0.006	
265.93	0.00	265.93	<0.015	Under 265.78-keV line, I_γ=0.04%
	35.843	230.09	<0.007	
	53.533	212.40	<0.008	
	65.475	200.46	<0.010	
	90.874	175.06	<0.003	
	112.954	152.98	<0.005	
	174.17	91.76	<0.0035	
	194.65	71.28	<0.004	
276.71	65.475	211.24	<0.008	
	112.954	163.76	<0.0014	
	174.17	102.54	<0.008	Under ^{153}Eu(n,γ) ^{154}Eu line
	194.65	81.74	<0.006	
321.11	65.475	255.63	<0.008	
	112.954	208.16	<0.003	
	174.17	146.94	<0.004	
	262.33	58.78	<0.003	
	265.93	55.18	<0.003	
	276.71	44.40	<0.002	
356.69	35.843	320.85	<0.07	Under strong 321.13-keV line
	112.954	243.74	<0.007	
	182.90	173.79	<0.006	Under 173.70-keV line, I_γ=0.014%.
	194.65	162.04	<0.010	Under 162.09-keV line, I_γ=0.027%.
	262.33	94.36	<0.0024	
	276.71	79.98	<0.0028	
362.29	112.954	249.34	<0.015	Between 249.14- and 249.93-keV lines
	182.90	179.39	<0.003	Under an impurity line at 179.43 keV
362.29	194.65	167.32	<0.005	
	262.33	99.96	<0.006	
	265.93	96.36	<0.004	
	276.71	85.58	<0.005	
	321.11	41.18	<0.003	
371.04	0.00	371.04	<0.008	
	7.535	363.50	<0.008	
	35.533	335.20	<0.011	
	53.533	317.51	<0.03	Under 317.80-keV line, I_γ=0.24%
	65.475	305.56	<0.006	
	90.874	280.17	<0.006	
	112.95	258.09	<0.006	
	127.298	243.74	<0.005	
	182.90	188.14	<0.028	Under 188.12-keV line
371.04	194.65	176.39	<0.006	
	265.93	105.11	<0.0005	
	276.71	94.33	<0.0024	
	321.11	49.93	<0.010	
405.46	0.00	405.46	<0.023	
	53.533	351.93	<0.011	
	65.475	339.99	<0.006	
	112.95	292.51	<0.006	
	174.17	231.29	<0.007	
	182.90	222.56	<0.1	Under 222.66-keV line, I_γ=0.24%
	194.65	210.81	<0.007	
	262.33	143.13	<0.007	
	265.93	139.53	<0.006	
	276.71	128.75	<0.006	
	321.11	84.35	<0.015	
	356.69	48.77	<0.010	
405.46	362.29	43.17	<0.005	
	371.04	34.42	<0.010	
414.91	53.533	361.38	<0.06	
	65.475	349.44	<0.010	Under wing of 349.16-keV line, I_γ=0.12%
	90.874	324.04	<0.008	
	112.95	301.96	<0.008	
	174.17	240.74	<0.012	
	182.90	232.01	<0.007	
	194.65	219.26	<0.007	
	262.33	152.55	<0.007	
	265.93	148.98	<0.007	
	356.68	58.23	<0.005	
	362.29	52.62	<0.008	
	371.04	43.87	<0.007	

assigned on the following assumptions: (1) The ground state is indeed $\frac{3}{2}^+$ (see Sec. IV A). (2) When states are connected by an $E1$ or $M1$ transition, then $\Delta J=0$ or 1. (3) When states are connected by an $E2$ transition, $\Delta J=0$ or 1 or 2. (4) When the K conversion coefficient is large enough that the transition is not likely to be pure $E2$, then $\Delta J=0$. or 1. (This includes the $E2+E0$ case, for which $\Delta J=0$.) (5) A transition from the $\frac{1}{2}^+$ neutron-capture state to a low-lying negative-parity state limits the spin of this state to $\frac{1}{2}^-$ or $\frac{3}{2}^-$. (6) A transition from the $\frac{1}{2}^+$ neutron-capture state to a positive-parity state limits the spin of the final state to $\frac{1}{2}^+$ or $\frac{3}{2}^+$ if the transition intensity is $>20\%$ of the average intensity of the other high-energy $M1$ transitions and to $\frac{1}{2}^+$, $\frac{3}{2}^+$, or $\frac{5}{2}^+$ if the high-energy transition is $<20\%$ of the average $M1$ intensity. This assumption is equivalent to saying that one expects that the primary $E2$ transition probabilities will be roughly a factor of 10–20 down from the average for $M1$ radiation, and hence that it is not likely that any $E2$ transition strengths will be as large as 20% of the $M1$ average value. This is consistent with the single-particle estimate for the $M1/E2$ intensity ratio $(\frac{1}{2}^+\rightarrow\frac{3}{2}^+)/(\frac{1}{2}^+\rightarrow\frac{5}{2}^+)=18/1$ for 6-MeV γ rays. The distribution of normalized intensities $I_\gamma E_0^3/E_\gamma^3$ for the high-energy transitions is plotted in Fig. 10. E_0 is the energy of the ground-state transition. Note that a subgroup in the $M1+E2$ section fits this description for $E2$ radiation. (7) When the intensity of a transition from the neutron-capture state to a negative parity state is $<0.3\%$ of the average intensity of transitions to the other negative-parity states, then $J\geq\frac{5}{2}$. (8) Since the population of a level is related to the spin of the level,[13] the intensity balance (Table XII of Sec. VI) gives some indication of the spin of a level.

Although the procedures for obtaining spin and parity assignments for many of the levels are quite similar, they will be discussed separately in Sec. IV to help the reader find specific information about an individual level. The subsection devoted to a level will also give some information about the interpretation of that level as a member of a rotational band. This is done by comparing the theoretical predictions of the Nilsson model[9,41] for the relative γ-ray transition strengths with the observed gamma intensities. The assignment of K values to the levels and the assignment of levels to possible rotational bands is discussed in detail in Sec. V. Some discussion is necessary in Sec. IV, however, if the reader is to understand the significance of the upper limits set on many of the missing γ transitions. These upper limits are much easier to interpret when they are compared with the intensities of γ transitions to levels in the same rotational band than when the comparison is with transitions proceeding to levels in different rotational bands. Usually, the absolute hinderance factors are quite similar for transitions to members of the same rotational band, but those for transitions to different rotational bands can differ by an order of magnitude or more.[42–46] This is especially true if some of the transitions are K-forbidden.

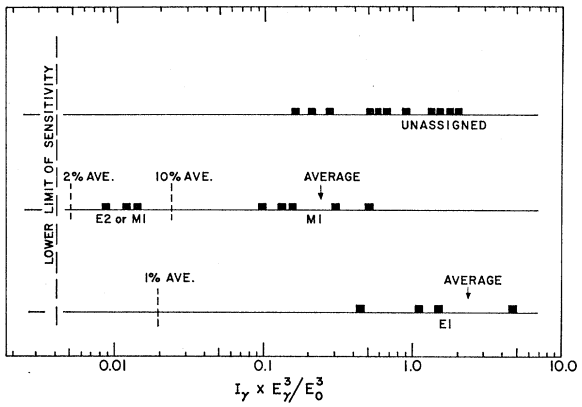

FIG. 10. Distribution of normalized γ intensities $I_\gamma E_0^3/E_\gamma^3$ for the high-energy transitions from the $\frac{1}{2}^+$ neutron-capture state to the low-lying levels in ^{153}Sm. E_0 is the energy of the ground-state transition. The lowest graph is for levels whose parity is opposite that of the ground state, the middle graph is for levels with the same parity, and the top graph is for transitions to levels with unassigned parity.

IV. DISCUSSION OF INDIVIDUAL LEVELS

A. Ground State ($\frac{3}{2}^+$)

The $\frac{3}{2}$ spin of the ground state is based on the atomic-beam magnetic-resonance work of Cabezas *et al.*[47] The positive parity assignment was initially based on the early (d, p) work,[7] in which the proton group to the ground state was found to be relatively weak. This low intensity required a $\frac{3}{2}^+$ assignment since the spectroscopic factor predicted for the most likely $\frac{3}{2}^-$ state, the one with $[Nn_z\Lambda]=[521]$, has the value $C_J^2=0.07$ to 0.105 (for $\delta=0.2$–0.3) while the spectroscopic factor for the $\frac{3}{2}^+$ [651] state is $C_J^2\approx 0$. As mentioned earlier, many of the spin and parity assignments made in the early (d, p) work[7] do not agree with our assignments. Thus it appeared important to check the $\frac{3}{2}^+$ assignment for the ground state.

As a further test of this positive-parity assignment, the relative intensities of the high-energy γ transitions from the neutron-capture state to the positive-parity (same parity as the ground state) states were compared with the intensities of similar transitions to the negative-parity (opposite parity from the ground state) states.

[41] B. R. Mottelson and S. G. Nilsson, Kgl. Danske Videnskab, Selskab, Mat.-Fys. Medd. **1**, No. 8 (1959); G. Alaga, K. Alder, A. Bohr, and B. R. Mottelson, *ibid* **29**, No. 9 (1955).

[42] M. N. Vergnes, Nucl. Phys. **39**, 273 (1962).

[43] A. K. Kerman, Kgl. Danske Videnskab. Selskab, Mat.-Fys. Medd. **30**, No. 15 (1956).

[44] A. Faessler, Nucl. Phys. **59**, 177 (1964).

[45] K. E. G. Löbner and S. G. Malmskog, Nucl. Phys. **80**, 505 (1966).

[46] A. Bohr and B. R. Mottelson, Atomnaya Energiya **14**, 41 (1967).

[47] A. Cabezas, E. Lipworth, R. Marrus, and J. Winocur, Phys. Rev. **118**, 233 (1960).

This comparison is shown pictorially in Fig. 10, in which each transition appears as a square in the histogram of events and the horizontal scale is the logarithm of the normalized γ intensity. The lowest graph is for the transitions to levels whose parity is opposite that of the ground state, the middle graph is for the transitions to levels with the same parity, and the top graph is for the transitions to levels with unassigned parity. The average value of the normalized intensity for the transitions to states with parity opposite that of the ground state is 8 times the average value for transitions to states with the same parity. This is consistent with the $E1$-multipole and negative-parity assignments for the "opposite" group and the $M1$ and positive-parity assignments for the "same" group.

The positive-parity assignment for the ground state has recently been confirmed by the average-resonance-capture work of Smither and Buss,[48] who used a technique developed by Bollinger *et al.*[49] This work, which measures the strength of the primary neutron-capture gamma rays when averaged over something like 200 neutron resonances, eliminates most of the Porter-Thomas-type fluctuation in the primary gamma strength associated with neutron capture in a single neutron resonance. Since all evidence presently available points to a positive parity assignment for the ground state of ^{153}Sm, we feel that it is reasonable to use this assumption in defining the parity of the rest of the levels in the scheme.

B. Level at 7.535 keV ($\frac{5}{2}^+$)

A comparison of the multipolarities of the transitions from other excited states to the 7.53-keV state and to the ground state ($\frac{3}{2}^+$) establishes that these two levels have the same parity. The observation of the weak γ transition from the $\frac{1}{2}^+$ neutron-capture state to this level limits the spin to $\leq\frac{5}{2}$ and favors the $\frac{5}{2}^+$ assignment because its intensity $I=0.014\%$ is only a twentieth of the average for the $M1$ transitions (as is seen in Fig. 10). The $J^\pi=\frac{1}{2}^+$ assignment is ruled out on the basis of transitions to this level from $\frac{5}{2}^-$ states in the level scheme at 90.974 and 182.90 keV. The connecting transitions from $\frac{3}{2}^+$, $\frac{5}{2}^+$, $\frac{7}{2}^+$, $\frac{3}{2}^-$, $\frac{5}{2}^-$, and $\frac{7}{2}^-$ states are consistent with the $\frac{5}{2}^+$ assignment.

As discussed in the following subsections, the γ decay of the seven levels at 35.843, 53.533, 90.874, 127.298, 174.17, 182.90, and 265.93 keV can all be understood in terms of the Nilsson model[9] for a single particle coupled to a deformed core if one assumes that the 7.53-keV level is the $\frac{5}{2}^+$ member of the $K=\frac{3}{2}$ rotational band built on the $\frac{3}{2}^+$ ground state. The major objection to this assignment is the relatively close level spacing of the $\frac{3}{2}^+$ and $\frac{5}{2}^+$ levels, which are only 7.53 keV apart. A more reasonable spacing based on the negative-parity bands might be about 40–60 keV. The close spacing could be explained if another $\frac{5}{2}^+$ state were found nearby in the level scheme. The interaction of the $\frac{5}{2}^+$ states could then be invoked to account for the depression of the 7.53-keV state to its observed position. The interaction would, of course, have to be a strong one. The recent (d, p) and (d, t) work[15] agrees with the $\frac{5}{2}^+$ assignment for the 7.53-keV state.

If one assumes a $\frac{3}{2}^+$ assignment for the 7.32-keV state, then the proposed spin assignments have to be changed for many of the levels (e.g., the 53.843- and 174.17-keV levels, among others) in Figs. 8 and 9 and the interpretation of the level scheme through the Nilsson model becomes more difficult. It would also be difficult to explain why the 7.53-keV level is not repelled more strongly by the $\frac{3}{2}^+$ ground state, and why many transitions are missing (e.g., the transition from the 174.17-keV state to the ground state). Table VI gives an upper limit $I_\gamma(\text{g.s.})/I_\gamma(7.53\text{ keV})\leq 0.001$ on the intensity of the 174.17-keV transition relative to that of the competing one ($E_\gamma=166.64$ keV) to the 7.53-keV state. Thus all the evidence points to a $\frac{5}{2}^+$ assignment for the 7.53-keV level.

C. Level at 35.843 keV ($\frac{3}{2}^-$)

The negative-parity assignment for the 35.84-keV level comes from the deduced $E1$ multipolarity the 35.84-keV transition ($E1$), which connects this level to the positive-parity ground state. The negative parity assignment is consistent with all of the multipole assignments in the level scheme. It has also been verified by the recent average-resonance-capture γ experiments by Smither and Buss.[48]

The spin of the level is limited to $\frac{1}{2}$ or $\frac{3}{2}$ by the strong transition from the $\frac{1}{2}^+$ capture state. The $\frac{1}{2}^-$ assignment is ruled out on the basis of transitions connecting it to $\frac{5}{2}^+$ and $\frac{7}{2}^-$ states. The interpretation of the early (d, p) work[7] disagreed with the $\frac{3}{2}^-$ assignment, but the later work[15] is in good agreement with it.

The logft value of the β transition from the $\frac{5}{2}^-$ ground state of ^{153}Pm[50] to this level is consistent with a $\frac{3}{2}^-$ assignment for this level, but would be in strong conflict with a $\frac{1}{2}^-$ assignment.

The 35.843-keV level decays to both the 7.53-keV level and the ground state. If one assumes that the 35-keV level is the band head of a $K=\frac{3}{2}$ rotational band and that the $\frac{5}{2}^+$ 7.53-keV state and the $\frac{3}{2}^+$ ground state are members of a $K=\frac{3}{2}$ rotational band, then the Nilsson model[50] predicts that the normalized intensities $I_N=\text{const}\times I_\gamma/E_\gamma{}^3$ of the 35.843- and 28.308-keV lines will be in the ratio $I_N(35.843)/I_N(28.308)=1.00/0.67$. This is in excellent agreement with the experimental ratio 1.00/0.69 given in Table VII and accords well with the later discussions (Secs. IV F and IV I) in

[48] R. K. Smither and D. J. Buss, Phys. Rev. (to be published).
[49] L. M. Bollinger and G. E. Thomas, Phys. Rev. Letters **18**, 1143 (1968); **21**, 233 (1968).
[50] Q. Nathan and S. G. Nilsson, in *Alpha-, Beta-, and Gamma-Ray Spectroscopy*, edited by K. Seighbahn (North-Holland Publishing Co., Amsterdam, 1965), Vol I, p. 601.

TABLE VII. A comparison between the observed γ-ray branching ratios for the levels at 35.84, 90.87, and 174.17 keV and the predicted ratios[a] based on pure Nilsson states. The constant in the normalized γ-ray intensity $I_N = \text{const} \times I_\gamma / E_\gamma^3$ is chosen so that $I_N = 1$ for one of the γ rays in each group of $E1$ or $M1$ transitions considered. The relative error in the last digit is given in parentheses. K, J^π, and E are the K value, spin and parity, and excitation energy (keV) of the level, respectively. The subscripts i and f refer to initial and final states, respectively. The theoretical predictions appear on the right. The labels $E1$, $M1$, and $E2$ refer to the multipolarity of the radiation.

Final state E_f	K_f	J_f^π	Normalized γ-ray intensity I_N of the transition from the initial state E_i: Experimental I_N	Theoretical predictions for different K_i and J_i^π					
			$E_i = 35.84$	$K_i =$	$\frac{3}{2}$		$\frac{1}{2}$		
			$J_i^\pi = \frac{3}{2}^-$	$J_i^\pi =$	$\frac{3}{2}^-$		$\frac{3}{2}^-$		
					$E1$		$E1$		
0.00	$\frac{3}{2}$	$\frac{3}{2}^+$	1.00		**1.00**		1.00		
7.53	$\frac{3}{2}$	$\frac{5}{2}^+$	0.69(6)		**0.67**		1.50		
			$E_i = 90.87$	$K =$	$\frac{3}{2}$		$\frac{1}{2}$		$\frac{5}{2}$
			$J^\pi = \frac{5}{2}^-$	$J_i^\pi =$	$\frac{5}{2}^-$		$\frac{5}{2}^-$		$\frac{5}{2}^-$
					$E1$		$E1$		$E1$
0.00	$\frac{3}{2}$	$\frac{3}{2}^+$	1.00		**1.00**		1.00		1.00
7.53	$\frac{3}{2}$	$\frac{5}{2}^+$	0.89(5)		**0.96**		6.85		0.43
53.53	$\frac{3}{2}$	$\frac{7}{2}^+$	1.33(13)		**1.78**		7.14		0.07
			$E_i = 174.17$	$K =$	$\frac{3}{2}$	$\frac{3}{2}$	$\frac{1}{2}$	$\frac{1}{2}$	$\frac{5}{2}$ $\frac{5}{2}$
			$J_i^\pi = \frac{7}{2}^-$	$J =$	$\frac{7}{2}^-$	$\frac{7}{2}^-$	$\frac{7}{2}^-$	$\frac{7}{2}^-$	$\frac{7}{2}^-$ $\frac{7}{2}^-$
					$E1$		$E1$		$E1$
0.00	$\frac{3}{2}$	$\frac{3}{2}^+$	<0.001		**0.00**		0.00		0.00
7.53	$\frac{3}{2}$	$\frac{5}{2}^+$	1.00		**1.00**		1.00		1.00
53.53	$\frac{3}{2}$	$\frac{7}{2}^+$	0.43(3)		**0.40**		4.45		0.71
(112.95)	$\frac{3}{2}$	$\frac{9}{2}^+$	(<0.08)		1.40		3.88		0.15
(65.47)			(<0.04)						
					$M1$	$E2$[b]	$M1$	$E2$[b]	$M1$ $E2$[b]
35.84	$\frac{3}{2}$	$\frac{3}{2}^-$	1.00		**0.00**	**1.00**	0.00	1.00	0.00 1.00
90.87	$\frac{3}{2}$	$\frac{5}{2}^-$	7.8(15)		**7.26**[c]	**0.54**	6.0–3.9[c]	1.8–3.9[d]	7.8[c] 0.01

[a] References 9 and 51.

[b] Adjusted for E_γ^5 energy dependence; the value of I_N is $(E_2/E_1)^2$ times the value given in Table XI.

[c] Adjusted so that $M1+E2$ is equal to the experimental value.

[d] A range of values are possible, as explained in Sec. V.

which the $\frac{5}{2}^-$ state at 90.874 keV and the $\frac{7}{2}^-$ state at 174.17 keV are assumed to be the next members of the same rotational band.

D. Level at 53.533 keV ($\frac{7}{2}^+$ or $\frac{5}{2}^+$)

The positive parity assignment for the 53.53-keV level is based on the L conversion coefficients ($M1$ or $E2$) of the 53.534- and 45.996-keV transition to the $\frac{3}{2}^+$ ground state and to the $\frac{5}{2}^+$ 7.53-keV state, respectively. The assignments of $\frac{1}{2}^+$ and $\frac{3}{2}^+$ are essentially ruled out by the lack of a primary gamma transition ($I_\gamma < 0.004\%$) from the $\frac{1}{2}^+$ capture state. The presence of connecting $E1$ γ rays to $\frac{5}{2}^-$, and $\frac{7}{2}^-$ states, and the lack of any connecting transition to either $\frac{1}{2}^-$ or $\frac{3}{2}^-$ states, supports this conclusion. The $\frac{7}{2}^+$ assignment is preferred to the $\frac{5}{2}^+$ assignment because no observed transition connects it to any of the states with $J^\pi = \frac{3}{2}^-$. Even after correcting for an E^3 energy dependence, the missing transition from the $\frac{3}{2}^-$ state at 127.29 keV to the 53.53-keV state has less than 0.006 of the strength of the transition to the $\frac{3}{2}^+$ ground state. This preference for the $\frac{7}{2}^+$ assignment over the $\frac{5}{2}^+$ is indicated in the level scheme (Figs. 8 and 9) by putting the $\frac{5}{2}$ assignment in parentheses.

If one assumes a $\frac{7}{2}^+$ assignment for this level, then the 53.53-keV transition to the $\frac{3}{2}^+$ ground state must be pure $E2$. Since it is similar in strength to the $M1$ transition to the ground state, suggestive of $E2$ enhancement, this level appears to be a good candidate for the $\frac{7}{2}^+$ member of the $K = \frac{3}{2}$ rotational band built on the $\frac{3}{2}^+$ ground state. The γ-ray branching ratios are shown in Table VIII.

An alternative interpretation would be to assume that the level is the $\frac{5}{2}^+$ band head of a $K = \frac{5}{2}$ rotational band. This level could then be used to help explain the downward displacement of the position of the $\frac{5}{2}^+$ 7.53-keV level discussed in Sec. IV B. The observed decay rates are quite different from any prediction based on a simple admixture of $K = \frac{3}{2}$ and $K = \frac{5}{2}$ for the 53.53-keV level. This does not, however, rule out a more complicated mixing involving other bands, which leads to the transition between the two proposed $\frac{5}{2}^+$ states being strongly enhanced relative to the $\frac{5}{2}^+ \rightarrow \frac{3}{2}^+$ transition.

E. Level at 65.475 keV

Direct measurement of a conversion coefficient for any of the transitions that connect the 65.47-keV level to the rest of the scheme was impossible because of their

TABLE VIII. A comparison between the observed γ-ray branching ratios for the levels at 53.53, 112.95, 65.47, and and 194.65 keV and the predicted ratios based on pure Nilsson states.[a] The notation is the same as in Table VII.

Final state E_f	K_f	J_f^π	Normalized γ-ray intensity I_N of the transition from the initial state E_i: Experimental I_N		Theoretical predictions for different K_i and J_i^π					
			$E_i=53.53$	$K_i=$	$\frac{3}{2}$	$\frac{3}{2}$	$\frac{5}{2}$	$\frac{5}{2}$	$\frac{3}{2}$	$\frac{5}{2}$
			$J_i^\pi=\frac{7}{2}^+$ or $\frac{5}{2}^+$	J_i^π	$\frac{7}{2}^+$	$\frac{7}{2}^+$	$\frac{7}{2}^+$	$\frac{7}{2}^+$	$\frac{5}{2}^+$	$\frac{5}{2}^+$
					$M1$	$E2$[b]	$M1$	$E2$[b]	$M1$	$M1$
0.00	$\frac{3}{2}$	$\frac{3}{2}^+$	1.0		**0.00**	**1.00**	0.00	1.00	1.00	1.00
7.53	$\frac{3}{2}$	$\frac{5}{2}^+$	3.0(3)		**1.89**[c]	**1.11**	**3.00**[c]	0.01	0.96	0.43
			$E_i=112.95$	$K_i=$	$\frac{3}{2}$	$\frac{3}{2}$	$\frac{3}{2}$	$\frac{5}{2}$	$\frac{3}{2}$	$\frac{5}{2}$
			$J_i^\pi=\frac{9}{2}^+$ or $\frac{7}{2}^+$ or $\frac{5}{2}^\pm$	$J_i^\pi=$	$\frac{9}{2}^+$	$\frac{9}{2}^+$	$\frac{7}{2}^+$	$\frac{7}{2}^+$	$\frac{5}{2}^+$	$\frac{5}{2}^+$
					$M1$	$E2$[b]	$M1$	$M1$	$M1$	$M1$
0.00	$\frac{3}{2}$	$\frac{3}{2}^+$	<0.15		**0.0**	**0.0**	0.0	0.0	1.00	1.00
7.53	$\frac{3}{2}$	$\frac{5}{2}^+$	1.0		**0.0**	**1.00**	1.00	1.00	0.96	0.43
53.53	$\frac{3}{2}$	$\frac{7}{2}^+$	9.0(18)		**8.7**[c]	**0.14**	0.40	0.71	1.78	0.07
			$E_i=65.47$	$K_i=$	$\frac{3}{2}$	$\frac{3}{2}$	$\frac{3}{2}$	$\frac{3}{2}$	$\frac{5}{2}$	
			$J_i^\pi=\frac{9}{2}^+$ or $\frac{7}{2}^+$ or $\frac{5}{2}^+$	$J_i^\pi=$	$\frac{9}{2}^+$	$\frac{7}{2}^+$	$\frac{7}{2}^+$	$\frac{5}{2}^+$	$\frac{5}{2}^+$	
					$E2$	$M1$	$E2$	$M1$	$M1$	
0.00	$\frac{3}{2}$	$\frac{3}{2}^+$	<0.05		0.00	0.00	1.00	1.00	1.00	
7.53	$\frac{3}{2}$	$\frac{5}{2}^+$	1.00		1.00	1.00	1.13	0.96	0.43	
			$E_i=194.65$	$K_i=$	$\frac{5}{2}$	$\frac{3}{2}$	$\frac{5}{2}$	$\frac{5}{2}$		
			$J_i^\pi=\frac{5}{2}^\pm$ or $\frac{7}{2}^+$	$J_i^\pi=$	$\frac{5}{2}^+$	$\frac{5}{2}^+$	$\frac{7}{2}^+$	$\frac{7}{2}^+$		
					$M1$	$M1$	$M1$	$E2$		
0.00	$\frac{3}{2}$	$\frac{3}{2}^+$	1.00		1.00	1.00	0.00	1.00		
7.53	$\frac{3}{2}$	$\frac{5}{2}^+$	0.42(12)		0.43	0.96	1.00	0.03		
53.53	$\frac{3}{2}$	$\frac{7}{2}^+$	<2.6		0.07	1.78	0.71	0.54		
(112.95)	$\frac{3}{2}$	$\frac{9}{2}^+$	<3.8		0.00	0.00	0.15	0.19		

[a] References 9 and 51.
[b] Adjusted for E_γ^5 energy dependence; the value of I_N is $(E_2/E_1)^2$ times the value given in Table XI.
[c] Adjusted so that $M1+E2$ is equal to the experimental value.

very weak intensities. It is possible, however, to set an upper and lower limit on the conversion coefficient of the weak 57.94-keV transition which depopulates the level. These limits, $3<I_e/I_\gamma<36$, for the K conversion line are most consistent with an $M1$ or $E2+M1$ multipole assignment. (See Table II for theoretical values.) The lower limit is much too large for an $E1$ assignment ($I_e/I_\gamma\approx0.1$) and the upper limit is too small for an $M2$ assignment ($I_e/I_\gamma\approx42$) or $E3$ ($I_e/I_\gamma\approx1200$) assignment. This analysis gives a positive parity assignment for the 65-keV level.

No primary transition was observed to this state ($I_\gamma<0.004\%$), so its spin is most likely $\geq\frac{5}{2}$. The high angular momentum of the incoming neutron ($l_n\geq3$) found for this level in the (d, p) work[7] likewise favors a high spin assignment. Transitions connect this level to other levels in the scheme with $J^\pi=\frac{5}{2}^+$ and $\frac{7}{2}^+$. These transitions limit the spin to $\leq\frac{9}{2}$ so the three most likely choices are $\frac{9}{2}$, $\frac{7}{2}$, and $\frac{5}{2}$. The low population of the level by the higher excited states suggests a spin higher than $\frac{5}{2}$.

The old (d, p) work[7] suggested an $\frac{11}{2}^-$ assignment for this level, while the new (d, p) work[15] favors a $\frac{9}{2}^+$ assignment.

F. Level at 90.874 keV ($\frac{5}{2}^-$)

The negative parity of the 90.87-keV level is based on the K-conversion coefficients of the 90.874-keV ($E1$) and 83.339 keV ($E1$) transitions to the positive-parity ground state and to the first excited state. The level is connected through gamma transitions to other levels in the scheme with assignments $J^\pi=\frac{3}{2}^+$, $\frac{5}{2}^+$, $\frac{7}{2}^+$, $\frac{3}{2}^-$, $\frac{5}{2}^-$, and $\frac{7}{2}^-$. This is consistent only with a $\frac{5}{2}^-$ assignment. The lack of any primary transition ($I_\gamma<0.004\%$) from the $\frac{1}{2}^+$ neutron-capture state supports this assignment. The old (d, p) work[7] suggested a $\frac{5}{2}^+$ assignment for this level, while the new (d, p) work[15] agrees with our $\frac{5}{2}^-$ assignment. The observation of a strong β transition to this level (as described in Sec. II E) from ^{153}Pm ($\frac{5}{2}^-$), $\log ft\approx5.8$, is consistent with the $\frac{5}{2}^-$ assignment.

The relative intensities of the γ rays to the lower levels suggest $K=\frac{3}{2}$ for this level if one assumes that the ground state, 7.53-keV state, and 53.53-keV state are the $\frac{3}{2}^+$, $\frac{5}{2}^+$, and $\frac{7}{2}^+$ members of a $K=\frac{3}{2}$ rotational band. The appreciable strength of the $M1(+E2)$ transition to the $\frac{3}{2}^-$ state at 35.84 keV suggests that these two states are members of the same rotational

TABLE IX. A comparison of observed γ-ray branching ratios for the 127.30-, 182.90-, and 265.93-keV levels with the predicted ratios based on pure Nilsson states.[a] The notation is the same as in Table VII.

Final state E_f	K_f	J_f^π	Normalized γ-ray intensity I_N of the transition from the initial state E_i Experimental I_N		Theoretical predictions for different K_i and J_i^π					
			$E_i=127.80$	$K_i=$	$\frac{3}{2}$	$\frac{3}{2}$	$\frac{1}{2}$	$\frac{1}{2}$		
			$J^\pi=\frac{3}{2}^-$	$J^\pi=$	$\frac{3}{2}^-$	$\frac{3}{2}^-$	$\frac{3}{2}^-$	$\frac{3}{2}^-$		
					$E1$		$E1$			
0.00	$\frac{3}{2}$	$\frac{3}{2}^+$	1.00		**1.00**		1.00			
7.53	$\frac{3}{2}$	$\frac{5}{2}^+$	0.52(3)		**0.67**		1.50			
53.53	$\frac{3}{2}$	$\frac{7}{2}^+$	<0.0006		**0.00**		0.00			
					$M1$	$E2$[b]	$M1$	$E2$[b]		
35.84	$\frac{3}{2}$	$\frac{3}{2}^-$	1.00		**1.00**	**1.00**	1.00	1.00		
90.87	$\frac{3}{2}$	$\frac{5}{2}^-$	0.41(8)		**0.67**	**0.40**	1.50	0.5–0.06[c]		
			$E_i=182.90$	$K_i=$	$\frac{3}{2}$	$\frac{3}{2}$	$\frac{1}{2}$	$\frac{1}{2}$	$\frac{5}{2}$	$\frac{5}{2}$
			$J^\pi=\frac{5}{2}^-$	$J^\pi=$	$\frac{5}{2}^-$	$\frac{5}{2}^-$	$\frac{5}{2}^-$	$\frac{5}{2}^-$	$\frac{5}{2}^-$	$\frac{5}{2}^-$
					$E1$		$E1$		$E1$	
0.00	$\frac{3}{2}$	$\frac{3}{2}^+$	1.00		**1.00**		**1.00**		1.00	
7.53	$\frac{3}{2}$	$\frac{5}{2}^+$	0.91(5)		**0.96**		6.85		0.43	
53.53	$\frac{3}{2}$	$\frac{7}{2}^+$	1.31(7)		**1.78**		7.14		0.08	
(112.95)	$\frac{3}{2}$	$\frac{9}{2}^+$	<0.09		**0.00**		0.00		0.00	
					$M1$	$E2$[b]	$M1$	$E2$	$M1$	$E2$
35.84	$\frac{3}{2}$	$\frac{3}{2}^-$	1.00		**1.00**	1.00	1.00	1.00	1.00	1.00
90.87	$\frac{3}{2}$	$\frac{5}{2}^-$	1.38		**0.96**	0.02	6.85	0.1–1.4[c]	0.43	1.48
			$E_i=265.95$	$K=$	$\frac{3}{2}$	$\frac{3}{2}$	$\frac{5}{2}$	$\frac{5}{2}$	$\frac{5}{2}$	$\frac{5}{2}$
			$J^\pi=\frac{7}{2}^-$ or $\frac{5}{2}^\pm$	$J^\pi=$	$\frac{7}{2}^-$	$\frac{7}{2}^-$	$\frac{7}{2}^-$	$\frac{7}{2}^-$	$\frac{5}{2}^-$	$\frac{5}{2}^-$
					$M1$	$E2$[b]	$M1$	$E2$[b]	$M1$	$E2$[b]
35.84	$\frac{3}{2}$	$\frac{3}{2}^-$	<1.3[d]		0.00		0.00		1.00	
90.87	$\frac{3}{2}$	$\frac{5}{2}^-$	<1.2[d]		1.00		1.00		0.96	
174.17	$\frac{3}{2}$	$\frac{7}{2}^-$	<1.1[d]		0.40		0.71		1.78	
127.80	$\frac{3}{2}$	$\frac{3}{2}^-$	1.0		**0.00**	**1.00**	0.00	1.00	1.00	1.00
182.90	$\frac{3}{2}$	$\frac{5}{2}^-$	13.1(13)		**12.0**[e]	**1.09**	13.1[e]	0.01	0.96	0.53

[a] References 9 and 51.
[b] Adjusted for E_γ^5 energy dependence.
[c] A range of values are possible.
[d] Normalized to the transition to the 127.80-keV level.
[e] Adjusted so that $M1+E2$ is equal to the experimental value.

band. Table VII compares this assignment with other possible choices. The energy spacing of the proposed $\frac{3}{2}^-$ and $\frac{5}{2}^-$ band members gives a rotational parameter $A=\frac{1}{2}\hbar^2\mathcal{I}=11.0$ keV, which is quite similar to the values found in other well-deformed nuclei of about the same mass.

G. Level at 112.954 keV

It was not possible to obtain meaningful upper or lower limits on the conversion-electron intensities of the 105.42- and 59.42-keV transitions that depopulate the 112.95-keV level, so no parity assignment can be made for it. γ rays connect it to lower levels with $J^\pi=\frac{5}{2}^+$ and $\frac{7}{2}^+$ and there is no direct transition from the $\frac{1}{2}^+$ neutron-capture state. This suggests $J^\pi=\frac{9}{2}^+$, $\frac{7}{2}^\pm$, or $\frac{5}{2}^\pm$. The 582.96-keV transition from the $J=\frac{1}{2}$ or $\frac{3}{2}$ level at 695.83 keV was not used in this analysis. The authors avoided the use of all transitions above 500 keV in arguments concerning the spin and parity of the levels below 500 keV. This was done to avoid basing a spin assignment on a γ ray which accidentally fitted into the level scheme. The complexity of the (n,γ) data increases with energy of the gamma ray while the resolution and precision decrease with the square of the energy. Thus the probability of this type of accidental fit is quite energy dependent. If the 582.96-keV transition is placed properly in the level scheme, then the $\frac{9}{2}$ assignment is unlikely, so only $J=\frac{7}{2}$ or $\frac{5}{2}$ is left.

On the other hand, the lack of transitions to the $\frac{3}{2}^+$ and $\frac{3}{2}^-$ states below it suggest that the $\frac{9}{2}^+$ or $\frac{7}{2}^+$ assignments are more likely. This state was not seen in the old (d,p) work[7] but is present in the new (d,p) work, where its weak population favors a $\frac{7}{2}^+$ or $\frac{9}{2}^+$ assignment.

The two transitions that depopulate this level proceed to the $\frac{5}{2}^+$ state at 7.53 keV and the $\frac{7}{2}^+$ (or $\frac{5}{2}^+$) state at 53.53 keV. If one assumes that the two lower states are the $\frac{5}{2}^+$ and $\frac{7}{2}^+$ members of a $K=\frac{3}{2}$ band built on the $\frac{3}{2}^+$ ground state, the relative intensities of the two transitions are consistent with the assignment of the 112.95-keV level as the $\frac{9}{2}^+$ member of this rotational band (as is indicated in Table VIII). Making this

assignment requires one to remove the conflicting 589.92-keV transition from the level scheme.

H. Level at 127.298 keV ($\frac{3}{2}^-$)

The negative parity of the 127.30-keV level is based on the multipolarities of the 127.298-keV ($E1$), 119.763-keV ($E1$), and 91.455 keV [$M1(+E2+E0)$] transitions to the $\frac{3}{2}^+$ ground state, the $\frac{5}{2}^+$ level at 7.53 keV, and the $\frac{3}{2}^-$ level at 35.843-keV level, respectively.

The strong transition ($I_\gamma=4.35\%$) from the $\frac{1}{2}^+$ neutron-capture state suggests a $\frac{1}{2}^-$ or $\frac{3}{2}^-$ assignment. The $\frac{1}{2}^-$ assignment is ruled out on the basis of transitions to and from states with $\frac{5}{2}^+$ assignments. The value $\log ft=5.1$ for the β transition to this level from ^{153}Pm ($\frac{5}{2}^-$) (Sec. II B) is consistent with $J^\pi=\frac{3}{2}^-$, but not with $J^\pi=\frac{1}{2}^-$.

The relative intensities of the γ transitions to the lower states suggest a $K=J=\frac{3}{2}$ negative-parity state. It is so listed in Table IX. This $\frac{3}{2}^-$ assignment agrees with both the new[15] and the old[7] (d, p) work.

I. Level at 174.17 keV ($\frac{7}{2}^-$)

The negative parity assignment for the 174.17-keV level is based on the $E1$ K conversion coefficient of the 166.64-keV transition to the $\frac{5}{2}^+$ state at 7.53 keV. The absence of any observable direct transition ($I_\gamma<0.004$) to this level from the neutron-capture state suggests a $J\geq\frac{5}{2}$ assignment. Transitions to and from states with $J^\pi=\frac{3}{2}^-$, $\frac{5}{2}^-$, $\frac{7}{2}^-$, $\frac{5}{2}^+$, and $\frac{7}{2}^+$ suggest a $\frac{7}{2}^-$ or $\frac{5}{2}^-$ assignment. The relatively weak population of this level from the higher excited states favors the higher spin. A special effort was made to observe the missing transition to the ground state. No trace of it was found and the very low upper limit $I_\gamma<0.001\%$ was set. The intensity of the observed transition to the $\frac{5}{2}^+$ first excited state is 1000 times this upper limit. If both the ground state and the first excited state are members of the same rotational band, then the retardation of $E1$ transitions to these two levels should be similar unless forbidden by spin selection rules, thus the $\frac{7}{2}^-$ assignment is much preferred to the $\frac{5}{2}^-$ assignment, as indicated in Table VII. This level is interpreted in Sec. V. of this paper as the $\frac{7}{2}^-$ member of a $K=\frac{3}{2}$ band built on the $\frac{3}{2}^-$ state at 35.84 keV. The value of the rotational parameter A obtained from the level spacing of the 35- and 90-keV suggests a $\frac{7}{2}$ member at 168 keV, which is reasonably close to the 174-keV excitation energy found for this state.

The old (d, p) work gave a $\frac{9}{2}^+$ assignment for this level but the new work favors a $\frac{7}{2}^-$ assignment.

J. Level at 182.90 keV ($\frac{5}{2}^-$)

The negative parity assignment for the level at 182.90 keV is based on the K conversion coefficients of lines to the lower levels. A $J\geq\frac{5}{2}$ assignment is suggested by the lack of a primary transition ($I_\gamma<0.005\%$) from the $\frac{1}{2}^+$ neutron-capture state. The strong transition to the $\frac{3}{2}^+$ ground state limits the spin to $J^\pi=\frac{5}{2}^-$ only. This is in good agreement with both the old and the new (d, p) work. The $\frac{5}{2}^-$ assignment is consistent with the $\log ft=5.8$ for the β transition to the level from ^{153}Pm ($\frac{5}{2}^-$).

The γ decay from this state to the lower levels is most consistent with a $K=\frac{3}{2}$ assignment and is therefore a good candidate for the $\frac{5}{2}^-$ state of the second negative-parity rotational band based on the $\frac{3}{2}^-$ state at 127.298 keV. The relevant intensity ratios are compared in Table IX. The energy difference of the $\frac{3}{2}^-$ and $\frac{5}{2}^-$ states gives the value $A=\hbar^2/2\mathcal{I}=11.12$ keV, which is very close to that of the first $\frac{3}{2}^-$ band.

K. Level at 194.65 keV

The existence of the 194.65-keV level was first suggested by the recent (d, p) work.[15] Only a few weak γ transitions connect it to the rest of the level scheme, so no parity assignment can be made for it. The fact that no transition to this level from the $\frac{1}{2}^+$ capture state was observed suggests that $J\geq\frac{5}{2}$. The transition to the $\frac{3}{2}^+$ ground state limits this assignment to $\frac{7}{2}^+$ or $\frac{5}{2}^\pm$. The weak population of this level from the higher excited states suggests that the higher spin ($\frac{7}{2}$) is more likely. There are so few transitions connecting this level to the rest of the scheme that it is difficult to be sure that the right γ rays have been chosen. The level appears as a dashed line in the level scheme to remind one of this uncertainty. It should be understood by the reader that we are not questioning the existence of the level but only our assignment of γ rays to depopulate it. The recent (d, p) work[15] suggests a $\frac{9}{2}^+$ assignment for this state.

L. Level at 262.33 keV

The positive parity of the 262.33-keV level is based on the $M1+E2$ character of the 254.794-keV transition to the first excited state ($\frac{5}{2}^+$). No primary transition connects this level to the $\frac{1}{2}^+$ capture state. There are observed decay transitions to levels with $J^\pi=\frac{3}{2}^+$, $\frac{5}{2}^+$, $\frac{7}{2}^+$, $\frac{5}{2}^-$, and $\frac{7}{2}^-$. These two facts limit the probable spin of the level to $\frac{7}{2}^+$ or $\frac{5}{2}^+$. The lack of a transition to or from any $\frac{3}{2}^-$ levels in the scheme, the very weak intensity of the 262.31-keV transition to the $\frac{3}{2}^+$ ground state, and the weak population of the level, strongly favor the $\frac{7}{2}^+$ assignment. This is in disagreement with the $\frac{7}{2}^-$ interpretation of both the new[15] and the old[7] (d, p) work but not with the actual l_n values observed in the experiments. It is quite possible that the neighboring level at 265.93 keV, which is discussed next, is the level seen in the charged-particle work.

The relative intensities of the γ rays connecting this state to the lower levels suggest a $\frac{7}{2}^+$, $K=\frac{3}{2}$ or $\frac{5}{2}$ assignment for the 262.33-keV level (as can be seen in Table X).

M. Proposed Level at 265.93 keV

Since the spin and parity assignment, $\frac{7}{2}^+$ or $\frac{5}{2}^+$, of the 262.33-keV level disagrees with the $\frac{7}{2}^-$ assignment sug-

TABLE X. Comparison of the observed and theoretical γ-ray branching ratios for some of the levels in ^{153}Sm above 200 keV. The notation is the same as in Table VII.

	Final state			Normalized γ-ray intensity I_N of the transition from the initial state E_i					
	E_f	K_f	J_f^π	Experimental I_N		Theoretical I_N			
				$E_i=262.33$	$K_i=$	$\frac{3}{2}$	$\frac{3}{2}$	$\frac{5}{2}$	$\frac{5}{2}$	$\frac{7}{2}$
				$J_i^\pi=\frac{5}{2}^+$ or $\frac{7}{2}^+$	$J_i=$	$\frac{7}{2}^+$	$\frac{7}{2}^+$	$\frac{7}{2}^+$	$\frac{7}{2}^+$	$\frac{7}{2}^+$
						$M1$	$E2^a$	$M1$	$E2^a$	$E2^a$
A	0.0	$\frac{3}{2}$	$\frac{3}{2}^+$	0.011(3)		0.0	0.71	0.0	31.0	1.59
	7.53	$\frac{3}{2}$	$\frac{5}{2}^+$	1.00		1.00	1.00	1.00	1.0	1.00
	53.53	$\frac{3}{2}$	$\frac{7}{2}^+$	0.42(6)		0.40	0.29	0.75	20.0	0.26
	(112.95)	$\frac{3}{2}$	$\frac{9}{2}^+$	(<0.13)		1.39	0.29	0.15	10.6	0.03
	(65.47)			(0.96)						
						$E1$		$E1$		$E1$
	35.85	$\frac{3}{2}$	$\frac{3}{2}^-$	<0.014		0.0		0.0		Forbidden
	90.87	$\frac{3}{2}$	$\frac{5}{2}^-$	1.00		1.00		1.00		
	174.17	$\frac{3}{2}$	$\frac{7}{2}^-$	2.2(7)		0.40		0.75		
	127.29	$\frac{3}{2}$	$\frac{3}{2}^-$	<0.009		0.0		0.0		
	182.90	$\frac{3}{2}$	$\frac{5}{2}^-$	1.00		1.00		1.00		
		$\frac{3}{2}$	$\frac{7}{2}^-$			0.40		0.75		
				$E_i=276.70$	$K_i=$	$\frac{3}{2}$	$\frac{3}{2}$	$\frac{1}{2}$	$\frac{1}{2}$	
				$J_i^\pi=\frac{3}{2}^+$	$J_i^\pi=$	$\frac{3}{2}^+$	$\frac{3}{2}^+$	$\frac{3}{2}^+$	$\frac{3}{2}^+$	
						$M1$	$E2^a$	$M1$	$E2^a$	
B	0.0	$\frac{3}{2}$	$\frac{3}{2}^+$	1.00		1.00	1.00	1.00	1.00	
	7.53	$\frac{3}{2}$	$\frac{5}{2}^+$	0.53(2)		0.67	2.40	1.50	0.1–1.1	
	53.53	$\frac{3}{2}$	$\frac{7}{2}^+$	0.30(2)		0.00	1.00	0.0	0.9–0.2	
	(112.95)	$\frac{3}{2}$	$\frac{9}{2}^+$	(<0.003)		0.0	0.0	0.0	0.0	
	(65.47)			(<0.001)						
						$E1$		$E1$		
	35.85	$\frac{3}{2}$	$\frac{3}{2}^-$	1.0		1.00		1.00		
	90.87	$\frac{3}{2}$	$\frac{5}{2}^-$	2.5(4)		0.67		1.50		
	174.17	$\frac{3}{2}$	$\frac{7}{2}^-$	<1.7		0.00		0.00		
	127.29	$\frac{3}{2}$	$\frac{3}{2}^-$	1.0		1.00		1.00		
	182.90	$\frac{3}{2}$	$\frac{5}{2}^-$	1.2(4)		0.67		1.50		
				$E_i=321.10$	$K_i=$	$\frac{1}{2}$	$\frac{1}{2}$	$\frac{3}{2}$	$\frac{3}{2}$	
				$J_i^\pi=\frac{3}{2}^+$	$J_i^\pi=$	$\frac{3}{2}^+$	$\frac{3}{2}^+$	$\frac{3}{2}^+$	$\frac{3}{2}^+$	
						$M1$	$E2^a$	$M1$	$E2^a$	
C	0.0	$\frac{3}{2}$	$\frac{3}{2}^+$	1.00		1.00	1.00	1.00	1.00	
	7.53	$\frac{3}{2}$	$\frac{5}{2}^+$	0.096(6)		1.50	0.1–1.1	0.67	2.43	
	53.53	$\frac{3}{2}$	$\frac{7}{2}^+$	0.010(2)		0.0	1.0–0.2	0.0	1.01	
	(112.95)	$\frac{3}{2}$	$\frac{9}{2}^+$	<0.004			0.0		0.0	
						$E1$		$E1$		
	35.85	$\frac{3}{2}$	$\frac{3}{2}^-$	1.00		**1.00**		1.00		
	90.87	$\frac{3}{2}$	$\frac{5}{2}^-$	1.40(28)		**1.50**		0.67		
	174.14	$\frac{3}{2}$	$\frac{7}{2}^-$	<1.1						
	127.29	$\frac{3}{2}$	$\frac{3}{2}^-$	1.00		**1.0**		1.00		
	182.92	$\frac{3}{2}$	$\frac{5}{2}^-$	1.10(20)		**1.50**		0.67		

TABLE X (*Continued*)

D			Experimental I_N for higher energy levels							
			E_i=356.69	362.29	405.46	414.91	447.07	450.04	481.08	630.20
			$J_i^\pi=\frac{5}{2}^+$	$\frac{5}{2}^+$	$\frac{3}{2}^-$	$\frac{1}{2}^+, \frac{3}{2}^+$	$\frac{5}{2}, \frac{7}{2}$	$\frac{5}{2}^-$	$\frac{3}{2}^+$	$\frac{3}{2}^-$
	E_f	K_f	J_f^π							
	0.0	$\frac{3}{2}$	$\frac{3}{2}^+$	1.0	1.00	<0.007	1.00	<0.17	<0.04	1.00	1.00
	7.53	$\frac{3}{2}$	$\frac{5}{2}^+$	2.9	1.34	1.00	0.06	1.00	1.00	2.8	0.80
	53.53	$\frac{3}{2}$	$\frac{7}{2}^+$	4.5	0.20	<0.005	<0.03	0.54	0.80	<0.04	<0.03
	35.84	$\frac{3}{2}$	$\frac{3}{2}^-$	<0.80	1.00	1.00	1.00		...	1.00	1.00
	90.87	$\frac{3}{2}$	$\frac{5}{2}^-$	1.00	0.67	0.53	<0.10		1.00	4.1	0.67
	174.17	$\frac{3}{2}$	$\frac{7}{2}^-$	1.50(20)	4.66	<0.08	<0.36		<0.9	<0.08	0.17
	127.30	$\frac{3}{2}$	$\frac{3}{2}^-$	1.00	1.00	1.00	1.00		<1.1[b]	<1.00	<1.42
	182.90	$\frac{3}{2}$	$\frac{5}{2}^-$	<1.7	<0.38	<1.4	<0.67		<1.0[b]	1.00	1.00

[a] Correction made for ratios of $E2$ transitions so that they can be compared with the experimental I_N values.

[b] Normalized to transition to the 90.87-keV level.

gested by the (d, p) work, an effort was made to find another level that would fit the $\frac{7}{2}^-$ assignment. The combination of γ rays and level energies used to suggest a level at 265.93 keV is the only obvious combination in this energy range. All of the γ rays involved are weak so no determination of the parity of this state could be made. The lack of a transition from the $\frac{1}{2}^+$ capture state, the weak population of the level, and the proposed transitions to levels with $J^\pi=\frac{5}{2}^+$, $\frac{3}{2}^-$, and $\frac{5}{2}^-$ are consistent with $J^\pi=\frac{7}{2}^-$ or $\frac{5}{2}^\pm$. The transitions to the $\frac{3}{2}^-$ state at 127.298 keV and the $\frac{5}{2}^-$ state at 182.89 keV make this level a good candidate for the $\frac{7}{2}^-$ member of a $K=\frac{3}{2}$ band built on the $\frac{3}{2}^-$ band head at 127.298 keV. The relative intensities of these two γ rays (Table IX) are consistent with this assignment. The simple rotational formula $E_L=E_0+AJ(J+1)$ predicts 261 keV for the energy of the $\frac{7}{2}^-$ member of the band. The level is dashed in the scheme (Fig. 8, 9) to remind the reader of its speculative character.

N. Level at 276.71 keV ($\frac{3}{2}^+$)

The positive parity of the 276.71-keV level is established by the K conversion coefficients of the two strong transitions to the $\frac{3}{2}^+$ ground state and the $\frac{5}{2}^+$ first excited state. The presence of a direct transition from the neutron-capture state and interconnecting transitions to levels with $J^\pi=\frac{3}{2}^+$, $\frac{5}{2}^+$, $\frac{7}{2}^+$, $\frac{3}{2}^-$, and $\frac{5}{2}^-$ is consistent only with a $\frac{3}{2}^+$ assignment. The relative intensities of transitions to the lower positive-parity levels (Table X) is most consistent with a $K=\frac{3}{2}$ assignment, while the γ intensities to the negative-parity levels suggest $K=\frac{1}{2}$.

O. Level at 321.11 keV ($\frac{3}{2}^+$)

The positive parity of the 321.11-keV state is based on the $M1$ K conversion coefficient of the strong 321.13-keV transition to the $\frac{3}{2}^+$ ground state. The direct transition from the $\frac{1}{2}^+$ neutron-capture state suggests a $\frac{1}{2}^+$ or $\frac{3}{2}^+$ assignment. The transition from this level to lower levels with spin $J^\pi=\frac{5}{2}^-$ and $\frac{7}{2}^+$ rule out the $\frac{1}{2}^+$ assignment.

The early (d, p) work[7] suggested a $\frac{5}{2}^-$ assignment for this level while the recent work[15] agrees with $\frac{3}{2}^+$ for the level.

The relative γ-ray intensities to the positive-parity levels do not correspond to any of the ratios predicted for pure Nilsson levels, while the transitions to negative-parity states are best fitted by a $K=\frac{1}{2}$ assignment.

P. Level at 356.69 keV ($\frac{5}{2}^+$)

The positive parity of the 356.69-keV is based on the $M1$ conversion coefficient of the 303.10-keV transition to the $\frac{7}{2}^+$(or $\frac{5}{2}^+$) level at 53.533 keV. The very weak ($I_\gamma=0.007$) primary transition is felt to be consistent with an $E2$ transition or a weak $M1$ transition. Therefore, the $\frac{5}{2}^+$ assignment as well as the $\frac{1}{2}^+$ and $\frac{3}{2}^+$ assignments must be considered. The transitions to the $\frac{5}{2}^-$ levels are used to rule out the $\frac{1}{2}^+$ assignment and the transitions to levels with $J^\pi=\frac{7}{2}^+$ and $\frac{7}{2}^-$ strongly favor the $\frac{5}{2}^+$ assignment over the $\frac{3}{2}^+$ assignment. The missing 320.85-keV transition to the $\frac{3}{2}^-$ state at 35.843 keV is most likely hidden under the very strong 321.13-keV line. The γ intensities to the lower positive-parity levels (Table X) might be explained by an admixture of $K=\frac{1}{2}$ and $K=\frac{3}{2}$. They do not match any of the ratios predicted for $M1$ by pure Nilsson states (Table XI). The transitions to the negative-parity states do not match the theoretical ratios for $E1$ transitions given in Table XI any better.

Q. Level at 362.20 keV ($\frac{5}{2}^+$)

The positive parity assignment for the 362.20-keV level is based on the K conversion coefficient of the strong 362.30- and 354.76-keV transitions to the ground state and first excited state. The relatively weak inten-

TABLE XI. Theoretical branching for normalized γ-ray intensities I_N calculated on the basis of the Nilsson model for deformed nuclei.[a] The notation is the same as in Table VII with the subscripts i and f denoting the initial and final states for the transition.

				$E1$ and $M1$ radiation				$E2$ radiation			
K_i	K_f	J_f	J_i	$\frac{1}{2}$	$\frac{3}{2}$	$\frac{5}{2}$	$\frac{7}{2}$	$\frac{1}{2}$	$\frac{3}{2}$	$\frac{5}{2}$	$\frac{7}{2}$
$\frac{1}{2}$	$\frac{1}{2}$	$\frac{1}{2}$		1.00	1.00				1.00	1.00	
$\frac{1}{2}$	$\frac{1}{2}$	$\frac{3}{2}$		2.0–0.5[b]	0.2–3.3	1.00		1.00	1.0–0.0	0.3–1.8	1.00
$\frac{1}{2}$	$\frac{1}{2}$	$\frac{5}{2}$			1.8–1.9	0.07–2.6	1.00	1.5–0.67	0.4–1.2	1.1–0.0	0.1–1.3
$\frac{1}{2}$	$\frac{1}{2}$	$\frac{7}{2}$				1.4	0.03–2.4		2.6–1.1	0.2–1.2	0.9–0.0
$\frac{3}{2}$	$\frac{1}{2}$	$\frac{1}{2}$			1.00				1.00	1.00	
$\frac{3}{2}$	$\frac{1}{2}$	$\frac{3}{2}$			0.80	1.00			4.0–1.0	0.07–4.4	1.00
$\frac{3}{2}$	$\frac{1}{2}$	$\frac{5}{2}$			0.20	1.15	1.00		3.9–0.4	0.6–5.6	0.2–4.1
$\frac{3}{2}$	$\frac{1}{2}$	$\frac{7}{2}$				0.35	1.33		1.1–0.08	1.4–2.7	0.4–6.1
$\frac{5}{2}$	$\frac{1}{2}$	$\frac{1}{2}$								1.00	
$\frac{5}{2}$	$\frac{1}{2}$	$\frac{3}{2}$								1.15	1.00
$\frac{5}{2}$	$\frac{1}{2}$	$\frac{5}{2}$								0.65	1.80
$\frac{5}{2}$	$\frac{1}{2}$	$\frac{7}{2}$								0.18	1.33
$\frac{1}{2}$	$\frac{3}{2}$	$\frac{3}{2}$		1.00	1.00	1.00		1.00	1.00	1.00	1.00
$\frac{1}{2}$	$\frac{3}{2}$	$\frac{5}{2}$			1.50	6.85	1.00	4.0–0.25	0.07–1.2	0.7–3.5	5.0–11.
$\frac{1}{2}$	$\frac{3}{2}$	$\frac{7}{2}$				7.14	4.45		1.4–0.3	0.4–3.5	1.7–38.
$\frac{3}{2}$	$\frac{3}{2}$	$\frac{3}{2}$			1.00	1.00			1.00	1.00	1.00
$\frac{3}{2}$	$\frac{3}{2}$	$\frac{5}{2}$			0.67	0.96	1.00		2.55	0.04	1.50
$\frac{3}{2}$	$\frac{3}{2}$	$\frac{7}{2}$				1.78	0.40		1.45	0.85	0.60
$\frac{5}{2}$	$\frac{3}{2}$	$\frac{3}{2}$				1.00				1.00	1.00
$\frac{5}{2}$	$\frac{3}{2}$	$\frac{5}{2}$				0.43	1.00			1.50	0.04
$\frac{5}{2}$	$\frac{3}{2}$	$\frac{7}{2}$				0.07	0.71			0.83	1.07
$\frac{7}{2}$	$\frac{3}{2}$	$\frac{3}{2}$									1.00
$\frac{7}{2}$	$\frac{3}{2}$	$\frac{5}{2}$									0.66
$\frac{7}{2}$	$\frac{3}{2}$	$\frac{7}{2}$									0.26
$\frac{1}{2}$	$\frac{5}{2}$	$\frac{5}{2}$						1.00	1.00	1.00	1.00
$\frac{1}{2}$	$\frac{5}{2}$	$\frac{7}{2}$							0.75	2.38	6.00
$\frac{1}{2}$	$\frac{5}{2}$	$\frac{9}{2}$								1.29	9.34
$\frac{3}{2}$	$\frac{5}{2}$	$\frac{5}{2}$			1.00	1.00	1.00		1.00	1.00	1.00
$\frac{3}{2}$	$\frac{5}{2}$	$\frac{7}{2}$				2.50	10.7		1.33	0.04	1.70
$\frac{3}{2}$	$\frac{5}{2}$	$\frac{9}{2}$					16.3			1.30	0.04
$\frac{5}{2}$	$\frac{5}{2}$	$\frac{5}{2}$				1.00	1.00			1.00	1.00
$\frac{5}{2}$	$\frac{5}{2}$	$\frac{7}{2}$				0.40	1.85			1.33	0.03
$\frac{5}{2}$	$\frac{5}{2}$	$\frac{9}{2}$					1.81			0.47	1.06
$\frac{7}{2}$	$\frac{5}{2}$	$\frac{5}{2}$					1.00				1.00
$\frac{7}{2}$	$\frac{5}{2}$	$\frac{7}{2}$					0.30				0.96
$\frac{7}{2}$	$\frac{5}{2}$	$\frac{9}{2}$					0.04				0.38

[a] References 9 and 51.

[b] A range of values are possible, as explained in Sec. V.

sity ($I_\gamma = 0.010\%$) of the primary transition from the $\frac{1}{2}^+$ capture state is felt to be consistent with either an $E2$ transition or a weak $M1$ transition. This allows a $J^\pi = \frac{1}{2}^+$, $\frac{3}{2}^+$, or $\frac{5}{2}^+$ assignment for the level. The presence of transitions to $\frac{5}{2}^-$, $\frac{7}{2}^-$, and $\frac{7}{2}^+$ states eliminates the $\frac{1}{2}^+$ and $\frac{3}{2}^+$ assignments and strongly suggests the $\frac{5}{2}^+$ assignment. Both the new[15] and the old (d, p) work[7] suggest $J \geq \frac{5}{2}$ for this level. Again the relative intensities of the γ rays to lower levels do not fit the pattern predicted by any single Nilsson level.

R. Level at 371.0 keV

The existence of the 371.04-keV level is based mainly on the charged-particle data[7,15] which suggest a high-spin level at 370.0 keV. The 371.0-keV level shown in Figs. 8 and 9 represents our attempt to identify the decay of this level in the (n, γ) data. Although the level fits all of the usual criteria (e.g., no primary transition, transitions only to other high-spin states, etc.), it cannot be considered uniquely established. A

weakly fed high-spin state might decay primarily through a single γ ray, e.g., through a transition to the next lower member of its rotational band. If the transitions to the other states were too weak to be seen, our level scheme would contain only one transition out of this level. Identifying this single γ ray would not be possible, of course, unless the precision of the (d, p) energy measurements were at least of the order of ± 0.5 keV, which is one half the average energy spacing between lines in this region of the γ spectrum. As in the case of the levels at 194.65 and 265.93 keV, this uncertainty in the (n, γ) analysis is indicated by dashing this state in the level scheme. This level is a possible candidate for the $\frac{9}{2}^-$ member of the $K=\frac{3}{2}$ negative-parity band based on the 127-keV level. Its energy (371 keV) is very close to the 370 keV which is predicted on the basis of the simple rotational formula $E_L=E_0+AJ(J+1)$, where A is calculated from the level spacing between the 174- and 265-keV levels.

S. Levels above 400 keV

The spin and parity assignments for the levels above 400 keV were obtained in the manner indicated in the previous discussions. Up to this point there has been essentially no conflict between the different kinds of evidence used to make these assignments. In most cases the choice of the gamma ray that best fitted into the level scheme was also clear cut. However, above 400 keV the level scheme becomes more complex and one begins to have to choose between different combinations of γ rays to depopulate the levels. The situation is most serious when there is no primary transition from the neutron-capture state to define the energy of the level. In the case of the two reported[7] high-spin levels at 501 and 548 keV, no obvious combination could be found; so no γ rays were assigned to these levels.

Table X lists the observed γ-ray branching ratios for some of these upper levels. The properties of these upper levels are discussed briefly in Sec. VI.

V. ROTATIONAL STRUCTURE OF LOW-LYING LEVELS

The two nearest neighbors of ^{153}Sm are the deformed even-Z even-N isotopes ^{152}Sm and ^{154}Sm. It is, therefore, quite reasonable to expect that ^{152}Sm might be described as an odd neutron coupled to a deformed core, as in the model proposed by Nilsson.[9] If the deformation of the ^{153}Sm core is similar to that found in its neighbors, ^{152}Sm and ^{153}Sm, then in the formula $E_J=E_0+AJ(J+1)$ for the level energies of the different members of a rotational band ($K\neq\frac{1}{2}$) the appropriate value for the rotational parameter $A=\hbar^2/2\mathcal{I}_0$ would be in the range 10–20 keV. This would correspond to an energy separation of 50–100 keV between the $J=\frac{3}{2}$ and $J=\frac{5}{2}$ members of a $K=\frac{3}{2}$ band. If the coupling of adjacent or overlapping rotational bands is not so strong as to completely destroy the expected sequence of level energies, then it should be possible to identify members of the same band from their energy spacings. This does indeed appear to be the case for the negative-parity levels below 400 keV which form two $K=\frac{3}{2}$ bands (35.843, 90.874, and 174.17 keV for the first and 127.289, 182.90, 265.93, and possibly 371.08 keV for the second) that have within 1 keV the same rotational-energy spacings. The values of the A parameter ($\approx$11 keV) for these two bands are quite consistent with the values found in other odd-A deformed nuclei in the same mass region. The $K=\frac{3}{2}$, positive-parity, rotational band proposed for the ground state ($\frac{3}{2}^+$) and the levels at 7.53 keV ($\frac{5}{2}^+$), 53.53 keV ($\frac{7}{2}^+$), and 112.94 keV ($\frac{9}{2}^+$) is, however, strongly distorted in that the 7.53-keV difference between the $\frac{3}{2}^+$ and $\frac{5}{2}^+$ states is much too small. The other spacings, however, agree with each other quite well and give a value $A\approx 6.6$ keV.

If one considers only pure Nilsson states, then the general expression for transition probabilities for γ rays between levels in different rotational bands is of the form[51]

$$T(M\lambda: J_iK_i\rightarrow J_fK_f)=\text{const}\times|\,C(J_i\lambda J_fK_f\,|\,J_iK_i\lambda K_f-K_i)+(-1)^{I-1/2+\lambda}\times\text{const}\times C(J_i\lambda J_fK_fJ_i-K_i\lambda K_f+K_i)\,|^2\times E_\gamma^{2\lambda+1},$$

where the C's are Clebsch-Gordan coefficients, λ is the multipolarity of the radiation, K_i and J_i are the K value and spin of the initial state, K_f is the K value of the final state, and J_f is the spin of the final state. The expression has two terms: The first is applicable when $\lambda\geq|K_i-K_f|$ and both are applicable when $\lambda\geq|K_i+K_f|$. The second term applies to the case of $M1$ or $E1$ radiation when $K_i=K_f=\frac{1}{2}$ and for $E2$ radiation when $K_i=\frac{1}{2}$, $K_f=\frac{3}{2}$, or $K_i=\frac{1}{2}$, $K_f=\frac{1}{2}$, or $K_i=\frac{3}{2}$, $K_f=\frac{1}{2}$. If one ignores these cases and restricts the radiation to one multipole, then the expression for the relative transition probabilities T_1 and T_2 can be reduced to the simple form

$$\frac{T_1}{T_2}=\frac{C_1(J_i\lambda J_fK_f\,|\,J_iK_i\lambda K_fK_i)^2}{C_2(J_i\lambda J_fK_f\,|\,J_iK_i\lambda K_fK_i)^2}\frac{E_{\gamma 1}{}^{2\lambda+1}}{E_{\gamma 2}{}^{2\lambda+1}}.$$

Selected experimental branching ratios are compared with the theoretical predictions in Tables VII–X. The boldfaced theoretical ratios are the ones we think best fit the data. Table XI gives a more complete set of theoretical values listed systematically in terms of K_i, K_f, and J_f for each J_i. The notation is the same as in Tables VII–X. In the majority of the cases considered, $\lambda<|K_i+K_f|$ and unique relative intensities can be calculated from the ratios of the squares of the appropriate Clobsch-Gordon coefficients. When $\lambda\geq$

[51] A. K. Kerman, in *Nuclear Reactions*, edited by P. M. Endt (North-Holland Publishing Co., Amsterdam, 1959), Vol. I, p. 427. See also Ref. 41.

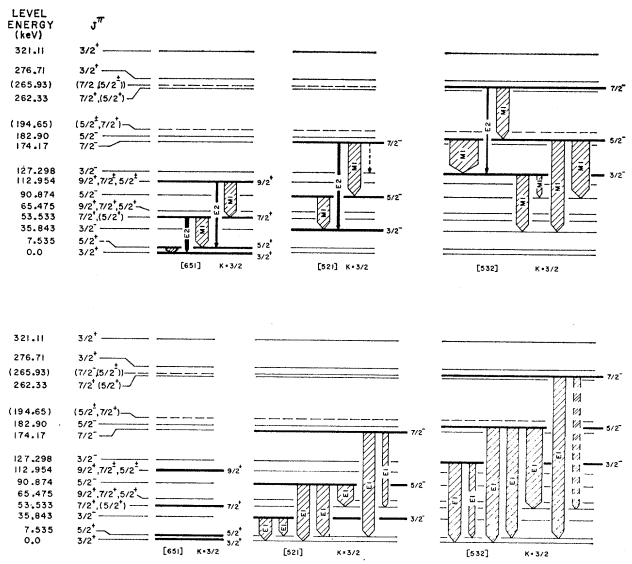

FIG. 11. Normalized γ decay of the low-lying rotational bands. Plot A shows the $M1$ and $E2$ transitions between levels with the same parity. Plot B shows $E1$ transitions between levels of different parity. The experimental values for the level energies (in keV) and for the spin and parity assignments are shown on the left. The proposed J^π assignments for the rotational bands are given to the right of each group. The width of each transition is proportional to its normalized γ intensity $I_N=\text{const}\times I_\gamma/E_\gamma{}^3$, given in Tables VII–IX. The labels on the transitions indicate the lowest possible multipole assignment that is consistent with the proposed spin and parity assignments. No transitions are left out. Dashed lines indicate "missing" transitions which may be hidden under lines of almost the same energy. The width of each dashed line represents the normalized upper limit of its intensity. The experimental upper limits on the normalized intensities of the other "missing" transitions are much smaller than these.

$|K_i+K_f|$, then the more general expression must be used for T_1 and T_2. The ratio is then given by

$$T_1/T_2=|C_1+bC_3|^2/|C_2+bC_4|^2,$$

where b is the ratio of the appropriate nuclear matrix elements and may be positive or negative. The value of b can be obtained from a detailed Nilsson-model calculation, but it requires one to specify which Nilsson orbitals are involved and to assume a value for the deformation parameter. What is given in the table instead are the two ratios: $|C_1|^2/|C_2|^2$ and $|C_3|^2/|C_4|^2$ which bracket the range of values possible when b is positive and give the appropriate ratios when $b\to 0$ and $b\to\infty$, respectively for both positive and negative values of b. This ambiguity in the theoretical predictions does not affect any of the discussions of $M1$ or $E1$ branching ratios presented in this paper because in all cases $K_f=\frac{3}{2}$ and therefore $|K_i+K_f|\geq 2$. By comparing the theoretical values quoted here with the experimental ratios given in Tables VII–IX, it is possible to determine how unique the proposed K-value assignments for the levels really are. Note that in some cases different assignments give similar intensity ratios. This means that it is the generally good fit for many of the ratios rather than any one ratio that makes the interpretation significant.

The level scheme of ^{153}Sm is redrawn in Fig. 11 to emphasize the different rotational bands. Part A shows the $M1$ and $E2$ transitions between levels in the same band and between levels in different bands with the same parity. Part B shows $E1$ transitions between levels of different parity. The experimental values for the level energies (in keV) and the spin and parity assignments from Fig. 8 are shown on the left. The proposed J^π assignments for the rotational-band members are given to the right of each group. The width of each transition is proportional to its normalized γ intensity $I_N=\text{const}\times I_\gamma/E_\gamma{}^3$, given in Tables VII–IX. The labels on the transitions indicate the lowest possible multipole assignment that is consistent with the proposed spin and parity assignments. No transitions are left out. The dashed lines indicate missing transitions which may be hidden under lines of almost the same energy. The width of each dashed line represents the normalized upper limit if its intensity. The experimental upper limits on the normalized intensities of the other missing transitions are much smaller than these. Note the similarity between the gamma decay patterns of the two negative-parity bands. This reflects the experimental conclusion that they are both $K=\frac{3}{2}$ bands. The decay patterns observed for transitions between members of the same band [Fig. 11, plot A] are quite similar for all three bands. The $M1/E2$ branching ratios appear to be normal for odd-N nuclei in this mass region.

The Nilsson diagram[52] for the energy of the odd

[52] The Nilsson level diagram used was based on the calculation of C. Gustafson, J. L. Lamm, B. Nilsson, and S. G. Nilsson (to be published). It is reproduced by C. M. Lederer, J. M. Hollander, and I. Perlman, *Table of Isotopes* (John Wiley & Sons, Inc., New York, 1967), 6th ed., Appendix V.

TABLE XII. List of the level energies and the spin and parity assignments for ^{153}Sm. These are followed by the proposed assignments for an interpretation of the level scheme based on the Nilsson Model. The last three columns give the sum of the intensities, $I_\gamma+I_{ce}$, going into the level or leaving the level, and the net difference, Out−In, in units of % of neutron-capture rate.

Level energy E (keV)	ΔE (keV)	Experimental assignment J^π	Proposed Nilsson model assignment J^π	K	$[Nn_z\Lambda]$	Intensity balance for level, $I_\gamma+I_{ce}$ In (%)	Out (%)	Diff. (%)
0.00		$\frac{3}{2}^+$	$\frac{3}{2}^+$	$\frac{3}{2}$	[651]	∼90.[a]	100.	∼10.[a]
7.535	0.005	$\frac{5}{2}^+$	$\frac{5}{2}^+$	$\frac{3}{2}$	[651]	34.	∼50.	∼16.[a]
35.842	0.005	$\frac{3}{2}^-$	$\frac{3}{2}^-$	$\frac{3}{2}$	[521]	8.58	14.30	5.82
53.533	0.005	$\frac{7}{2}^+$, $(\frac{5}{2}^+)$	$\frac{7}{2}^+$	$\frac{3}{2}$	[651]	2.98	8.44	5.46
65.475	0.005	$\frac{9}{2}^+$, $\frac{7}{2}^+$, $\frac{5}{2}^+$				0.87[b]	0.04[b]	−0.83[b]
90.874	0.005	$\frac{5}{2}^-$	$\frac{5}{2}^-$	$\frac{3}{2}$	[521]	1.79	7.10	5.31
112.954	0.010	$\frac{9}{2}^+$, $\frac{7}{2}^\pm$, $\frac{5}{2}^\pm$	$(\frac{9}{2}^+)$[c]		[651][c]	0.28[b]	0.05[b]	−0.23[b]
127.298	0.005	$\frac{3}{2}^-$	$\frac{3}{2}^-$	$\frac{3}{2}$	[532]	5.04	14.66	9.62
174.17	0.01	$\frac{7}{2}^-$	$\frac{7}{2}^-$	$\frac{3}{2}$	[521]	0.45	1.43	0.98
182.90	0.01	$\frac{5}{2}^-$	$\frac{5}{2}^-$	$\frac{3}{2}$	[532]	1.14	4.31	3.17
(194.65)[d]	0.01	$(\frac{5}{2}^+, \frac{7}{2}^+)$				0.17[b]	0.03[b]	−0.14[b]
262.33	0.02	$\frac{7}{2}^+$, $(\frac{5}{2}^+)$				0.30	0.98	0.68
(265.93)[d]	0.02	$(\frac{7}{2}^-, (\frac{5}{2}^\pm))$	$\frac{7}{2}^-$	$\frac{3}{2}$	[532]	0.17	0.25	0.08
276.71	0.02	$\frac{3}{2}^+$				>0.37[e]	3.23	<2.86[e]
321.11	0.02	$\frac{3}{2}^+$				0.55	3.23	2.68
356.69	0.02	$\frac{5}{2}^+$				0.12	0.79	0.67
362.29	0.02	$\frac{5}{2}^+$				0.03	2.16	2.13
(371.04)[d]	0.02	$(\frac{9}{2}, \frac{7}{2})$	$\frac{9}{2}^-$	$\frac{3}{2}$	[532]	0.0	0.52	0.52
405.46	0.05	$\frac{3}{2}^-$				0.52	3.97	3.45
414.91	0.05	$\frac{1}{2}^+$, $\frac{3}{2}^+$				0.26	3.48	3.22
447.07	0.05	$\frac{5}{2}$, $\frac{7}{2}$				0.0	0.39	0.39
450.04	0.05	$\frac{5}{2}^-$				0.0	1.47	1.47
481.08	0.04	$\frac{3}{2}^+$				0.41	∼2.9[e]	∼2.5[e]
524.36	0.06	$\frac{5}{2}$				0.0	1.16	1.16
629.90	0.12	$\frac{3}{2}^{(-)}$				1.08	3.81	2.23
695.83	0.15	$\frac{1}{2}^{(+)}$, $\frac{3}{2}^{(+)}$				0.61	2.63	2.01
734.90	0.15	$\frac{5}{2}$				0.04	2.96	2.92
750.32	0.15	$\frac{1}{2}$, $\frac{3}{2}$				0.40	2.99	2.59

[a] This value is only approximate because of the large uncertainty in the intensity of the 7.53-keV line.
[b] This value is based on the sum of only the γ intensities.
[c] Some of the experimental evidence conflicts with this assignment.
[d] Parenthesis indicate levels which are dashed in the level scheme.
[e] Uncertainty in sum due to uncertainty in position of 473-keV γ ray.

neutron as a function of the deformation suggests two possible asymptotic assignments for the $\frac{3}{2}^+$ ground state with 91 neutrons: either [651] or [402]. The former corresponds to a deformation parameter value $\epsilon=0.19$–0.24 and the later to $\epsilon=0.35$–0.38. The recent (d, p) work[15] suggest that the most likely assignments for the $K=\frac{3}{2}$ negative-parity bands are [521] and [532] for the 35.84- and 127.30-keV band heads, respectively. The small energy separation of the two band heads would appear to favor the smaller value of the deformation parameter given above.

The weak proton group to the ground state in the (d, p) reaction[7,15] favors the [651] assignment. This configuration will mix strongly with [660] and [642] configurations through the Coriolis interaction because they are all part of the $i_{11/2}$ shell. This Coriolis coupling between the levels may be sufficient to explain the strong distortion of the ground-state band. Putting reasonable parameters into the appropriate theoretical expressions[53,54] suggests that the interaction could be strong enough to move the levels 50–100 keV even if the interfering levels were several hundred keV higher in energy. No detailed calculations were made in this work, mainly because of the uncertainty of the spin assignment of the two closest unassigned levels at 65.47 and 194.65 keV and also because of the large choice of possible interfering states. It is, of course, possible that this low-lying positive-parity group is some other complex structure whose branching ratios are similar to those of a rotational band. Another alternative would be to assume that the 7.53-keV state is the $\frac{5}{2}^+$ band head of a new rotational band (e.g., $K=\frac{5}{2}$, [642]) with the states at 53 and 112 keV as the next two members. Adjustment of the band mixing might

[53] P. O. Tjøm and B. Elbek, Kgl. Danske Videnskab. Selskab, Mat.-Fys. Medd. **36**, No. 8 (1967).
[54] B. E. Chi, Nucl. Phys. **83**, 97 (1966).

bring about a fit to both the level energies and the γ-ray branching ratios, but this has not been demonstrated.

As one moves up in the level scheme, the γ-ray branching ratios look less and less like transitions between pure Nilsson levels. This is to be expected. The level scheme becomes quite complicated, with many levels of the same spin and parity quite close in energy. The resulting mixing between states with different K values could presumably account for most of the observed intensity ratios. Another interesting change occurs in the γ-ray branching ratios for these higher-energy states. The relative intensities of the $M1$ and $E2$ transitions from the positive-parity states to the ground-state rotational band are much stronger than the competing $E1$ transitions to the two low-lying negative-parity bands. Just the reverse (the expected situation) is true for the γ rays proceeding from the upper negative-parity bands. To put it another way, there is a general preference for transitions to the low-lying positive-parity levels over transitions to the negative-parity levels, the average transition strength of the favored transitions being ten times that of the hindered group. (The high-spin states with uncertain parity were not included in this analysis.) Some of this difference may be explainable in terms of the selection rules of Alaga[55] for changes in the asymptotic quantum numbers $[Nn_z\Lambda]$; but the trend seems too general for this to account for all of the effect. The major exception to the rule is the state at 695 keV ($J=\frac{1}{2}$ or $\frac{3}{2}$) that decays predominantly to the first $\frac{3}{2}^-$ state at 35 keV.

VI. CONCLUSIONS

Much new information about the level scheme of ^{153}Sm has been developed in this paper. 37 levels have been established below 1.4 MeV, many of which were unobserved previously. Parity assignments have been made for 17 of these levels. Unique spin assignments have been made for 14 of these levels and narrow limits have been placed on the spin assignments of the remaining states. Table XII lists these level energies and their errors along with the proposed J^π, K, and $[Nn_z\Lambda]$ assignments for the 28 levels below 800 keV (see Table IV for information on higher energy levels). Table XII also lists the total incoming and outgoing transition strengths and the net difference between these two values. This difference reflects the missing transition strength associated with the rest of the level scheme.

Ten of the first 14 levels below 300 keV can be interpreted as members of three low-lying rotational bands. All three bands appear to be $K=\frac{3}{2}$ and their band heads are the $\frac{3}{2}^+$ ground state, the $\frac{3}{2}^-$ level at 35.843 keV, and the $\frac{3}{2}^-$ level at 127.298 keV. The strong distortion of the ground-state band in this picture suggests strong Coriolis coupling to a nearby $K=\frac{5}{2}$ band. The level spacing of the two negative-parity bands follows the $J(J+1)$ rule quite well and in each case suggest a value $A=11$–12 keV, where $E_J=E_0+AJ(J+1)$. The logft values (Sec. II E) obtained for the β transitions from the $\frac{5}{2}^-$ [532] ground state of ^{153}Pm to these negative-parity levels are in good agreement with the proposed spin and parity assignment as well as with the suggested [521] and [532] assignments for their respective asymptotic quantum numbers.

The good agreement between the observed γ-ray intensity ratios and the theoretical predictions based on pure Nilsson states may be related to the fact that all these bands have $K=\frac{3}{2}$. The change in K for all transitions is therefore $\Delta K=0$, which usually results in more predictable intensity ratios for $E1$ transitions.[41–45] Also, any mixing of the two negative-parity bands does not introduce a different value of K. Hence all parts of the wave function still correspond to $K=\frac{3}{2}$ and do not, therefore, lead to a change in the intensity ratios for transitions with single multipolarity.

Although some features of the gamma decay of the upper levels may suggest the presence of additional rotational band structure, more detailed calculation involving Coriolis coupling are needed before any further conclusions can be drawn as to the applicability of the model. The somewhat surprising fact that in the decay of many of the higher-energy positive-parity levels, the $M1$ transitions to the low-lying states are appreciably stronger than the competing $E1$ transitions may be explained by these more detailed calculations once the character of these upper states is better defined.

ACKNOWLEDGMENTS

The authors wish to thank George Thomas and James Specht for their assistance in taking the high-energy Ge(Li) detector data. The authors also wish to thank R. K. Sheline for supplying them with information on the new (d, p) and (d, t) data before it was published. The authors wish to express their appreciation to Allen Magruder for his assistance in analyzing the bent-crystal and Ge(Li) data. We thank Professor H. Maier-Leibnitz for support and interest, Professor P. Kienle, Professor H. J. Mang, Dr. O. Schult, Dr. H. Vonach, and Dr. W. Nörenberg for discussions, Dr. J. Fink and W. Berger for help, and the Leibnitz-Rechenzentrum der Bayerischen Akademie der Wissenschaften for computer time.

[55] G. Alaga, Nucl. Phys. **4**, 625 (1957).